Alma Mater Studiorum – Università di Bologna

DOTTORATO DI RICERCA IN
BIOLOGIA CELLULARE E MOLECOLARE

Ciclo XXVI

Settore Concorsuale di afferenza: 05/E2

Settore Scientifico disciplinare: BIO/11

Titolo Tesi

Staphylococcus aureus bones and joints infections:
in vivo studies and host immune response

Presentata da: Alessia Corrado

Coordinatore Dottorato	**Relatori**
Ch.mo Prof. Vincenzo Scarlato	**Dott. Giuliano Bensi**
	Dott. Emiliano Chiarot
	Ch.mo Prof. Vincenzo Scarlato

Esame finale anno 2014

Il mio progetto di dottorato, presentato in questo lavoro di tesi, è stato focalizzato sul settaggio di un modello animale di artrite/osteomielite mediate da *Staphylococcus aureus*, che nell'uomo è il batterio maggiormente responsabile di queste gravi e debilitanti patologie. Queste malattie sono difficili da trattare anche per la costante crescita di Stafilococchi multi resistenti agli antibiotici (MRSA) e attualmente nessun vaccino contro questo batterio è disponibile sul mercato.

Il modello settato è riproducibile e duraturo e mima ciò che avviene nell'uomo, con le due classiche fasi di infezione: la fase acuta e quella cronica. Nel presente lavoro è stata studiata la risposta immunitaria dell'ospite durante tutte le fasi della patologia, sia considerando ciò che avviene nel sito di interesse (articolazioni del ginocchio) sia la situazione sistemica.

Questo modello è stato inoltre utilizzato per testare l'efficacia di un vaccino contro *S. aureus* proposto da Novartis.

I risultati di tale studio sono riportati nella seguente tesi.

TABLE OF CONTENTS

1 Introduction

1.1 *Staphylococcus aureus*

Staphylococcus was first isolated in 1880 in United Kingdom, by the surgeon Sir Alexander Ogston in pus from a surgical abscess in a knee joint (1). *Staphylococcus aureus* is a facultative anaerobic Gram-positive coccus, member of the *Firmicutes*, also known as "golden staph" and "Oro staphira". *S. aureus* appears as grape-like clusters when observed through a microscope, and it has large, round, golden-yellow colonies, often surrounded by a hemolytic halo, when grown on blood agar plates (2).

S. aureus is the most prevalent specie of staphylococci that leads Staph-mediated infections. It frequently colonizes different body districts such as nares, axilla, vagina, pharynx and skin. It has been reported that 20% of the human population are long-term carriers of *S. aureus* and worldwide approximately 30-50% of the healthy adults are colonized at any time point during their life (3).

Although *S. aureus* is not always pathogenic, *S. aureus* disease-associated strains are often able to promote infections by, for example, producing potent protein toxins, and expressing cell-surface proteins that bind and inactivate antibodies (4, 5).

Methicillin-resistant *Staphylococcus aureus* (MRSA) resistant strains have become resistant to most widely used β-lactam antibiotics.

MRSA strains are most often found associated with institutions such as hospitals, but are also becoming very common in community-acquired infections (6).

There are many clinical manifestations of staphylococcal infections, ranging from skin and soft tissues diseases to the most invasive pathologies represented by the metastatic infections and endocarditis (7, 8, 9, 10, 11).

In most cases infections occur after breaches of the skin or mucosal barriers through wounds, trauma or surgical intervention that allow the organism to access the tissues or the bloodstream; once the skin or mucosa have been penetrated, the infection may spread to the blood causing invasive diseases. Figure 1 reports the different staphylococcal diseases, arranged on the basis of their frequency and severity (12).
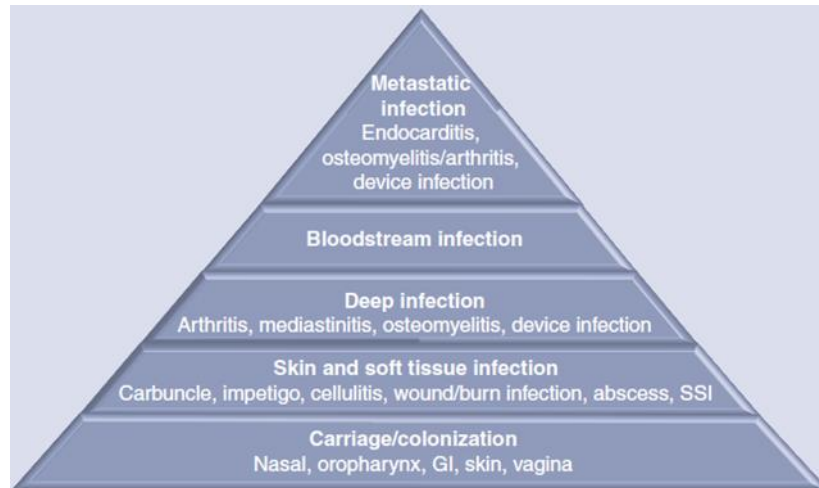
Figure 1: *S. aureus* **diseases**

The pyramid reports the broad spectrum of *Staphylococcus aureus* diseases. The severity of them decreases from top to bottom, on the other end the frequency decreases from bottom to top.

Adapted from "Strategies for and advances in the development of *Staphylococcus aureus* prophylactic vaccines"; Jane Broughan et al. 2011

1.2 *Staphylococcus aureus* joints and bones infections

Staphylococci are the principal causative agents of two major types of bones infections, septic arthritis and osteomyelitis, which involve the inflammatory destruction of joints and bones. These diseases lead serious morbidity and are often difficult to treat (13). The most common routes of infection for both septic arthritis and osteomyelitis are either haematogenous, resulting from bacteremia, contiguous, when the infection is transmitted from local tissue, or direct, resulting from infiltration of bone, often following surgeries, injuries, or implantations of a foreign body, for example joint replacement (13,

14, 15, 16, 17). Among the possible routes of infection most septic joints develop as a result of hematogenous seeding of the vascular synovial membrane due to a bacteremic episode (18,19). Infections may result in acute or chronic forms and affect native joints, especially knee and hip, or prosthetic joints, long bones, vertebrae and almost any other bone. The incidence of septic arthritis is between 2 and 10 in 100,000 in the general population but it may be as high as 30–70 per 100,000 in rheumatoid arthritis sufferers or recipients of prosthetic joints (15, 20, 21) and it is more common in children than adults, and in males than in females (22). Haematogenous osteomyelitis usually effects children and elderly people (17) and in children the incidence is between 1 in 5000 and 1 in 10,000 (23). Local spread of infection from contiguous tissue to bone or direct infection can occur at any age, with foreign body implants representing an important risk factor (17). The presence of an implant is frequently associated with chronic osteomyelitis, where antibiotic treatment is often ineffective, and removal of the implant and debridement are required (14). Some cases of relapsing osteomyelitis with several decades between subsequent episodes have been documented, and there are records of reactivation fifty or even eighty years after the first infection (14, 24, 25). *Staphylococcus*, principally *S. aureus,* accounts for between 37% and 67% of septic arthritis isolates as resulting from studies carried out in a range of nations (15, 26, 27, 28).
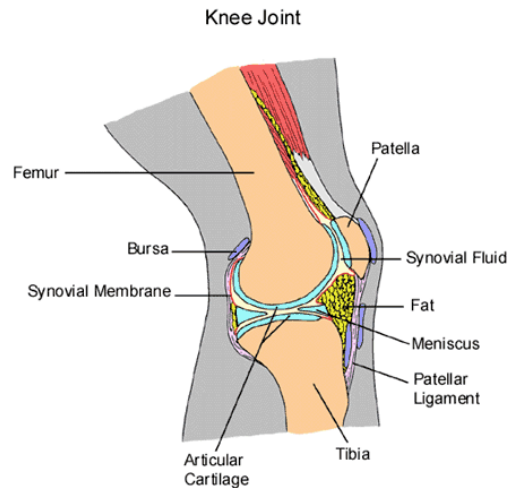
Figure 2: **Knee joint anatomy**

From:http://www.practical-wellness-guide.com/physical/total-personal-health-care-and-wellness

Septic arthritis is a joint pathology characterized by bacterial colonization and fast articular destruction (22). Inflammation with infiltration of leukocytes into the joint fluid is the result of bacterial growth within the synovium (15, 20). The production of bacterial toxins, host matrix metalloproteinases (MMPs) and reactive oxygen species and lysosomal enzymes, promote the destruction of cartilage. This latter process, mediated by polymorphonuclear leukocytes, begins with degradation of host proteoglycans followed by collagen breakdown within a few hours after the infection. The containment of the inflammation within the joint results in increasing pressure which prevents blood and nutrient supply to the joint increasing joint damage (15, 20, 29, 30).

Osteomyelitis includes a range of infections in which bacteria colonize bone with associated inflammation and bone destruction. Acute osteomyelitic foci are characterized by pus-forming inflammation at the site of microbial colonization. Damage to bone matrix, compression and destruction of vasculature is also observed as the infection spreads to surrounding soft tissues, which can further exacerbate bone necrosis (16, 17). Sections of dead bone, known as *sequestra*, may then detach resulting in separate infectious foci which, due to the lack of vasculature, are protected from immune cells and antibiotics (16,17). Such areas of dead, infected tissues that are inaccessible to the immune response or antimicrobials can lead to chronicization of the infection (16).

The infection by *S. aureus* is accompanied by a rapid recruitment of polymorphonuclear granulocytes and activated macrophages that are then followed by T cells. Although monocytes and macrophages are important to clear bacteria, they also play a pivotal role in the destructive inflammation within the joint (13). Moreover, a number of host cytokines play a significant role in the pathogenesis of osteomyelitis and arthritis, and there is strong evidence that production of these cytokines is induced by staphylococcal infection of bone and joints, and that they directly contribute to bone destruction. In particular, the inflammatory cytokines tumor necrosis factor α (TNFα), interleukin 1 (IL-1) and IL-6 seem to be especially important in bone physiology and pathology (32). In patients with

acute osteomyelitis, plasma levels of TNFα, IL-1β (the secreted form of IL-1) and IL-6 are all elevated (32, 33). High levels of IL-1β, IL-6 and TNFα are also found in the synovial fluid of patients with septic arthritis (34, 35). The local source of these cytokines is not fully understood. Production of IL-1β can be induced in human osteoblast-like cell lines by a variety of stimuli, including TNFα (36). Infiltrating immune cells may therefore be a more likely source of IL-1β and TNFα in bone in response to infection (37, 38, 39, 40). Moreover IL-6 is produced by osteoblasts in response to a variety of signals, including infection with *S. aureus* (37, 38). In addition to staphylococcal induction of inflammatory mediators that modulate the actions of osteoblasts and osteoclasts, bacteria of this genus are involved in more direct interactions with bone cells. Invasion and persistence of *S. aureus* in 'non-professional phagocytic' host cells *in vitro* has been described for many different cell types, including epithelial cells, endothelial cells and keratinocytes (41, 42). Electron microscopy has demonstrated the presence of bacteria within osteoblasts and osteocytes of embryonic chicks following injection with *S. aureus,* indicating that internalization by bone cells could also occur *in vivo* (43). The internalization of *S. aureus* by bone cells *in vivo* provides a protective niche for the bacterium, where it is shielded from immune effector mechanisms and antibiotics may help to explain persistent cases of osteomyelitis. Increasing evidence supports the importance of staphylococcal surface components as

virulence determinants by enabling initial colonization. In a number of studies, mutations in these surface receptors strongly reduced the ability of staphylococci to produce infection. In a murine septic arthritis model, inoculation of mice with a strain mutated in the collagen adhesin gene showed that septic arthritis occurred 43% less often than in the corresponding wild type (44). Also vaccination with a recombinant fragment of the *S. aureus* collagen adhesin was able to reduce the sepsis-induced mortality rate to 13%, compared to 87% of the control group (45). Nevertheless, the role of collagen adhesion of *S. aureus* as a major virulence factor has recently been questioned since approximately 30 to 60% of clinical isolates do not display collagen binding *in vitro* or the cna-encoded collagen adhesin (46). Staphyloccal fibronectin binding proteins (FbpA and FbpB) may also play a major role in the colonization and virulence of septic arthritis. In a recent study all the tested clinical isolates (n = 163) contained one or both of the coding regions for these binding proteins and 95% of these strains had a comparable fibronectin binding capacity to that seen in a staphylococcal reference strain known to efficiently bind fibronectin (47). These receptors may play an additional role in an intracellular immune-avoidance strategy. *S. aureus* survives intracellularly after internalization by cultured osteoblasts (48). Initial adherence to cells is mediated by *S. aureus* fibronectin receptors (49) possibly using fibronectin as a bridge between the host cell and the bacterial receptors. Following adherence, bacteria may be

internalized by host mechanisms involving membrane pseudopod formation (seen in established bovine mammary epithelial cell lines) or through receptor-mediated endocytosis via clathrin-coated pits (seen in mouse osteoblasts and epithelial cells, 49, 50).

Following internalization, staphylococci may induce apoptosis via a host caspase-dependent mechanism or survive intracellularly (49, 51, 52, 53). Induced apoptosis may exacerbate the host cell damage seen in septic arthritis. Moreover, staphylococci may escape clearance by the immune system and antimicrobial therapy by persisting within these host cells. This survival was recently demonstrated *in vivo* when *S. aureus* cells were found in the cytoplasm of embryonic chicken osteoblasts and osteocytes in mineralized bone matrix (43). In another study, *S. aureus* was found within polymorphonuclear neutrophils in an infection model, and these infected host cells were able to establish infection in naïve animals (54). Therefore, this pathogen may utilize invasion as an immune avoidance technique during the host inflammatory response. Following the down regulation of the adaptive immune response through T-cell apoptosis (mediated by superantigens, other toxins, and invasion), fulminant and/or persistent infection may result.

Antibiotic therapy during septic arthritis is efficacious only when rapidly applied and, often, in combination with joint drainage (29). The antibiotic therapy is based on appropriate culture and antibiotic sensitivity results (55).

Osteomyelitis, on the contrary, results often refractory to antibiotic treatment, a problem exacerbated by the increasing levels of antibiotic resistance among *Staphylococcus* spp. This is further complicated by the emergence of particularly persistent, antibiotic-resistant 'small colony variant' forms that may be selected for by certain current treatment regimens (14, 56, 57). Staphylococcal bone infections are thus likely to be a continuing and probably increasing problem, and the understanding of host-pathogen interactions in bones and joints will become crucial for the development of novel therapeutic and preventing strategies.

1.3 Novartis proposed Combo vaccine

The treatment of staphylococcal infections in the last years has been complicated also by the emergence of multidrug resistant strains, which can cause invasive diseases that frequently lead to death. Presently,no vaccines are available to prevent this kind of infections. Novartis Vaccines & Diagnostic (NVD) has engaged in the research and development of an effective vaccine against *S. aureus* infections. Using different approaches, including reverse vaccinology, proteomic and comparative genomics analyses (58), Novartis selected a combination of four highly conserved antigens, which were proposed as components of a potential innovative multiprotein-based vaccine. The vaccine formulation is composed of two surface proteins FhuD2, and Sur 2, and three secreted proteins, a toxoid derivative of α-

Hemolysin (Hla) (H35L) and EsxA-B, a fusion protein of two secreted toxins.

Hla is a pore-forming toxin whose expression is associated with staphylococcal pneumonia in mice and humans (59). Its expression is up-regulated in exponential phase and consistently expressed by clinically relevant strains. The protein included in the vaccine carries a substitution of histidine 35 with leucine that produced a mutant toxin (H35L) without hemolytic or lethal activity (60). EsxA-B derives from the fusion of the proteins EsxA and EsxB, both of them being expressed by clinically relevant strains and involved in abscess formation (61). FhuD2 is a lipoprotein involved in iron uptake, up regulated in iron deplete-conditions (58). Finally Sur 2 is a protein of still unknown function. This antigen combination has been tested using different animal models of *S. aureus* infections (pneumonia, abscess and sepsis model), resulting protective in all the cases and effective in preventing the infections carried out by different *S. aureus* strains.

1.4 Aim of the project

Since the relative importance of *S.aureus* mediated joints and bones infections both in terms of frequency and severity (fig. 1), the aim of this work was the development of an animal model of septic arthrosynovitis and osteomyelitis resembling the natural disease in humans and suitable for testing preventive and therapeutic tools. The hematogenous source of infection (intravenous inoculation) was preferred among the others due to its higher frequency of occurrence in humans. Our attention was focused to track in the long term bacterial infiltration in joints and bones using different microbiological and histopathological tools, which could allow us to have a complete overview of the situation and to understand the mechanisms set up by the host to contain or eradicate bacterial infection. Antibodies response, cytokines profiles during the time and cellular recruitment were therefore monitored for a period that allowed us studying both acute and chronic phases of these diseases *in situ*. The systemic infection and the host immune response were also evaluated. Finally the Novartis proposed vaccine against *S. aureus* diseases was tested in the model of acute infection, and bacterial reduction *in situ* and systemically was evaluated and compared to a standard antibiotic prophylaxis.

Having a powerful tool to study specific bacterial mediated diseases is nowadays an important requirement for the scientific community to shed light on the complex interactions between host and pathogens

and to test treatments for preventing or contrasting infections. We believe that our work could improve the knowledge in the field of *S. aureus* dependent pathologies, opening the possibility for further investigations in several fields of study.

2 Results

2.1 *S. aureus* shows a particular tropism for bones and joints causing both arthrosynovitis and osteomyelitis in mice

Since *S. aureus* was demonstrated to have a particular tropism for bones and joints in humans during natural infections (13), we started analyzing the interaction between pathogen and host infecting mice with bioluminescent bacteria. Bioluminescence (BLI) has been used as a powerful tool for studying host-pathogen interactions for years (62) and nowadays many different *S. aureus* bioluminescent strains are available on the market (Perkin Elmer). Many of them were generated using a plasmid (pXEN5, Perkin Elmer) carrying the *Photorhabdus luminescens* lux operon (figure 3), which allows random integration of lux genes into either the bacterial chromosome or natural plasmids carried by the pathogen. Once integrated in bacterial DNA downstream of a functional promoter, this operon is able to make bacteria bioluminescent without the need of extra sources of substrates (fig.3). The lux operon is a 9-kilobase fragment of the *Photorhabdus luminescens* genome that controls bioluminescence through the catalyzation of the enzyme luciferase (Meighen, 1991). The lux operon has a known gene sequence of luxCDAB(F)E, where lux A and lux B code for the components of luciferase, and the lux CDE codes for a fatty acid reductase complex

that makes the fatty acids necessary for the luciferase mechanism (63). Lux C codes for the enzyme acyl-reductase, lux D codes for acyl-transferase, and lux E makes the proteins needed for the enzyme acyl-protein synthetase. Luciferase produces blue/green light through the oxidation of reduced flavin mononucleotide and a long-chain aldehyde by diatomic oxygen. The reaction is summarized below (Silverman et al., 1984): $FMNH_2 + O_2 + R\text{-}CHO \rightarrow FMN + R\text{-}COOH + H_2O + Light$.
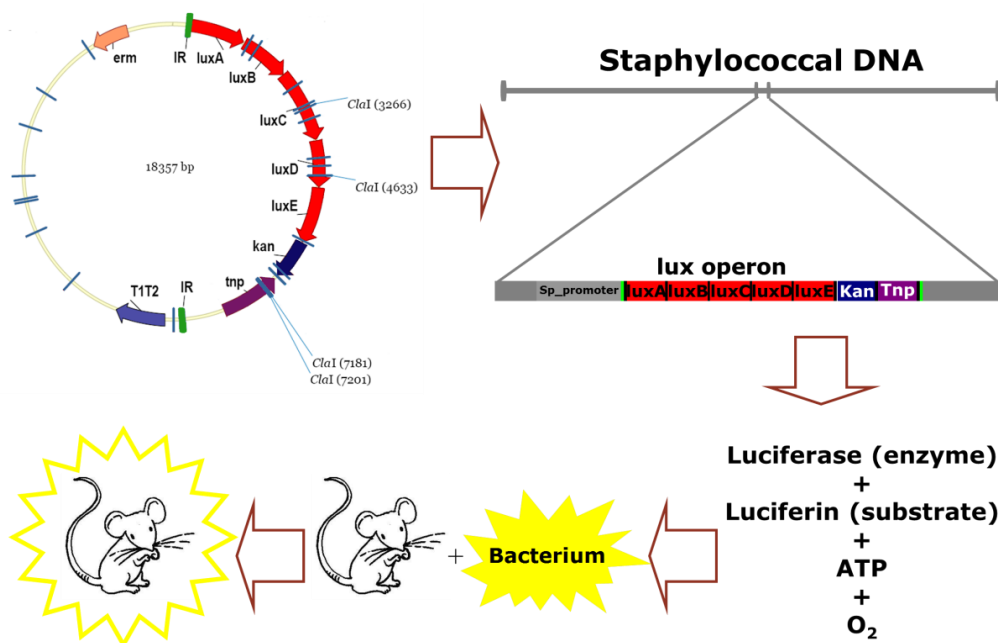
Figure 3. Generation of bioluminescent bacteria using the pXEN5 random integration system. pXEN5 plasmid used for random integration of *Photorhabdus luminescens* lux operon in DNA of recipient bacteria and mechanism of action of the inserted lux operon. luxA-E are lux genes, Kan is the resistance for the antibiotic kanamycin.

The light produced by this enzymatic reactions is captured by special imaging systems, in our case IVIS100 and IVIS Spectrum-CT, which exploit a special cooled camera enclosed in a light-proof box to capture all the photons emitted by the live mouse. Bioluminescent spots from the mouse body can be related to specific body areas and the intensity of the light emitted can be quantified.

The bioluminescent strains we used and their features in term of integration are reported here below in figure 4.

S. aureus Bioluminescent bacteria:

Xen 8.1 (NCTC 8325) ⎫
                          ⎬ Chromosome integration
Xen 29 (ATCC12600) ⎭

Xen 36 (ATCC 49525) ⎬ Plasmid integration

Figure 4. List of bioluminescent *S. aureus* used for *in vivo* imaging studies. Parenteral strains are reported in the brackets and whether the lux operon was inserted inside the chromosome or into a stable native plasmid is reported on the right.

All the strains used were highly bioluminescent and suitable for *in vivo* studies, as reported in the site

http://www.perkinelmer.com/Catalog/Family/ID/Gram%20Positive.

S. aureus bioluminescent strains were therefore used to infect mice in the lateral tail vein (i.v.) and infection progression was followed for at least 1 week after the injection using an IVIS 100$^{®}$ machine

(Perkin Elmer). The i.v. route of infection was chosen trying to mimic a hematogenous source of infection, often occurring in humans. As reported in figure 5A, 1 day after injection *S. aureus* reached the knee joints being able to establish a local infection that persisted for at least 7 days. Bioluminescence values, expressed as photon/second, (p/s) were calculated considering only our region of interest (ROI) reported as red circle in figure 5A, and a very good correlation could be observed when BLI was compared to colony forming units (CFUs) counted after knee joint washes the last day of the experiment (fig. 5B). Similarly to what obtained for Xen 36 strain, when other *S. aureus* strains were used to infect animals (fig. 5C) bacteria rapidly and lastingly localized in the joints, underlying that all the different *S. aureus* strains we tested had the ability to reach this body district. Finally we confirmed the presence of bacteria in knee joints after i.v. inoculation using confocal microscopy, as reported in figure 5D.
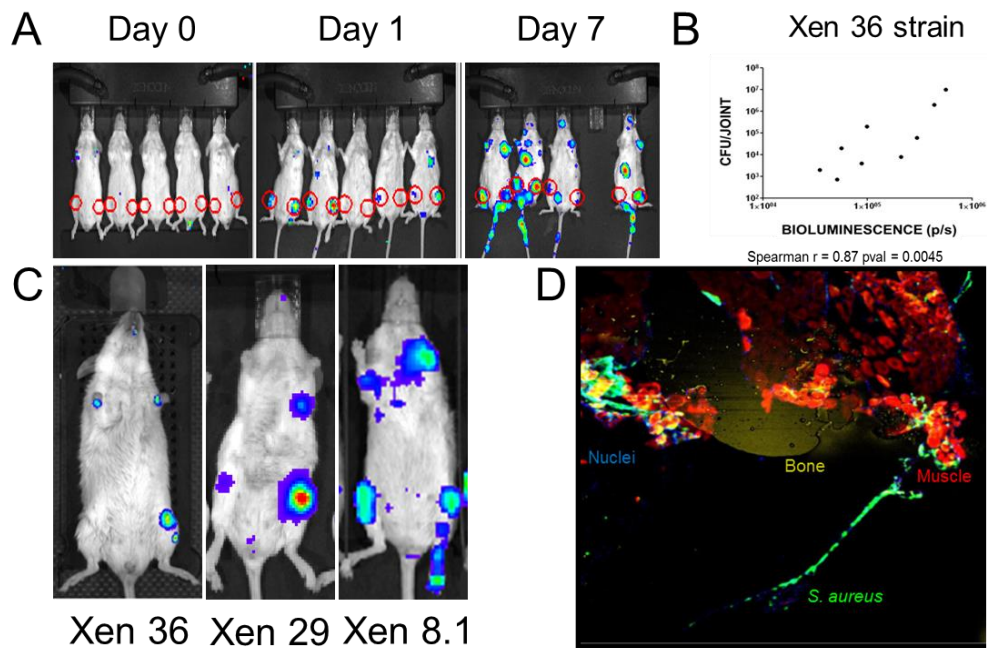
Figure 5. *Staphylococcus aureus* showed a particular tropism for joints in a mouse model of intravenous infection. A) Bioluminescence observed during the time from day 0 through day 7 in mice intravenously infected with *S. aureus* Xen 36 strain (1×10^7 CFU/mouse). In red, Region Of Interest (ROI) used to quantify the signal. B) A good correlation expressed as Spearman R value was measured when bioluminescence in the selected ROIs was compared to CFU recovered in knee joint washes of animals infected with Xen 36 strain. C) Signals observed at different time points using 3 *S. aureus* bioluminescent strains commercially available. *S. aureus* tended to localize in joints. D) Confocal microscopy analysis of a mouse knee from an infected animal. In yellow: bone (osteocalcin), in red: muscle (phalloidin), in blue: nuclei (dapi), in green: *S. aureus*

Since in humans *S. aureus* is able to cause osteomyelitis, we used the *in vivo* imaging approach also to better understand whether

bacteria which had reached the joint could invade the bone tissue. Mice were again i.v. infected with the highly bioluminescent strain Xen 36 and then followed for 1 week post infection. Using the IVIS spectrum-CT system$^{®}$ which combines a camera able to acquire bioluminescent signals and a tomography system that can scan sections of the animal body, we found that bioluminescent bacteria were not only present in the knee joint area but also in the tibia. This is shown in figure 6 where the 2D (A) and the 3D (B) analysis of the same infected animal are reported.
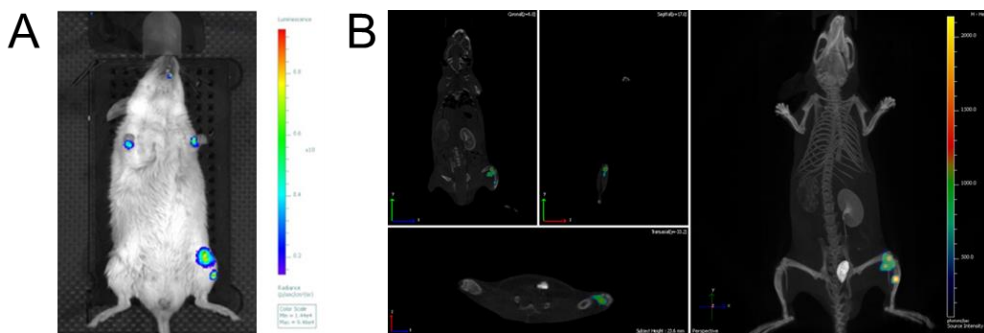
Figure 6. *Staphylococcus aureus* **was localized both in knee joints and bones.** A) 2D bioluminescent acquisition of a CD1 mouse i.v. infected with Xen 36 *S. aureus* strain. Two bioluminescent signals were detected in the left leg. B) 3D analysis of the same animal. The 2 bioluminescent signals turned to be one in the knee joint and the other in the left tibia. In both the cases an IVIS spectrum-CT system® was used to acquire images.

These findings allowed us to confirm that *S. aureus*-mediated hematogenous infection could cause arthrosynovitis and osteomyelitis, nevertheless, to better characterize bacterial

localization and local damages we carried out histopathological analysis of tissues obtained from infected mice. One week after infection with *S. aureus* Newman strain, mice were sacrificed, knees were removed, fixed and tissue slices were prepared. Hematoxylin and Eosin (H&E) staining were performed and histopathological analysis of these preparations was compared to slices derived from joints and bones of not infected mice. As shown in figure 7A on the right (red-framed image), when animals were infected with *S. aureus* the normal architecture of bones and joints was effaced by the presence of mixed inflammatory cells (with prevalence of neutrophils and macrophages) as compared with a control animal on the left (black-framed image). In particular, the tibia was destroyed and granulomas/abscesses were observed. Periostal inflammation was severe, causing thickening of the periostal tissue. Inflammation was evident in the synovia, which appeared severely thickened. In the enlargement, elongated cells can be seen which formed a wall around foci of inflammation composed by neutrophils and macrophages. Within the inflammatory focus, clusters of bright pick eosinophylic slightly hyaline material consistent with the presence of bacteria were observed. Indeed, immune-histochemical staining demonstrated that *S. aureus* was present in bone abscesses (figure 7B_1) and a wall of neutrophils was built up all around these structures (fig. 7B_3).
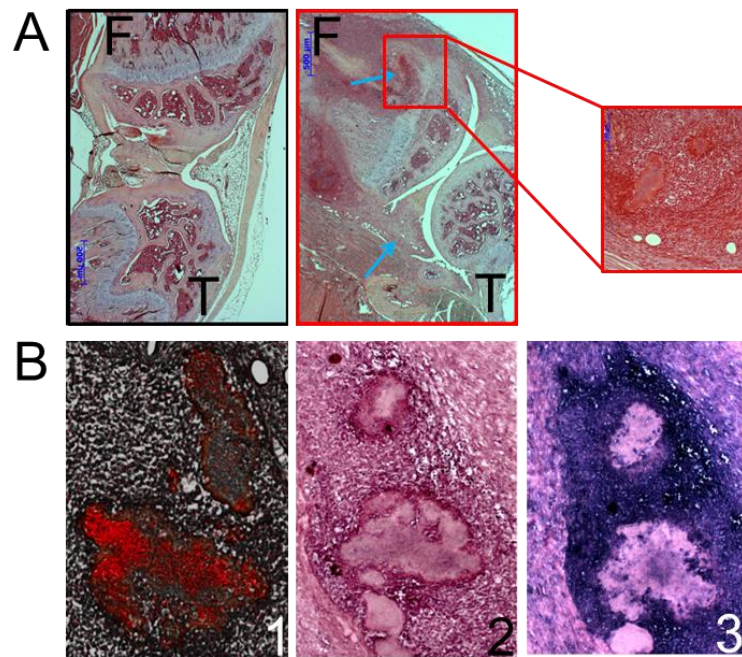
Figure 7.*Staphylococcus aureus* was responsible for causing arthritis and osteomyelitis in mice. A) Hematoxylin and Eosin (H&E) staining of mouse legs i.v. infected with *S. aureus* Newman strain. On the left (surrounded with a black frame) a slice from a not infected animal is reported as negative control, while on the right (red frame) a slice from a mouse infected and sacrificed 1 week after injection is reported. F= Femur T= Tibia. The smallest panel is an enlargement of a specific area of the red-frame image. B) Immune-histochemistry staining of knees from animals treated intravenously with *S. aureus*. In B1) *S. aureus* was stained in red (this antibody recognizes soluble and structural antigens of *Staphylococcus aureus* whole bacterium) in B3) neutrophils were marked in violet (the antibody recognizes a currently undetermined structure on the neutrophil membrane). B2) is the isotype control of B3.

2.2 Setting up of an arthrosynovitis mouse model of infection suitable for long lasting *in vivo* studies

2.2_1 CFU counts and histological analysis

For the setting up of a long lasting and reproducible mouse model of hematogenous *S. aureus*-mediated arthrosynovitis Xen 36 did not appear to be a suitable strain. In fact, the infectious dose required to be able to follow *in vivo* a detectable bioluminescent signal was too high and mice showed several signs of disease after the first week from the infection. The *S. aureus* Newman strain was therefore chosen for these experiments since it has been largely used in research worldwide being well adapted for animal studies. The first objective was to find a dose high enough to homogeneously infect a group of mice both systemically and in the knee joints, but reducing the risk of causing severe disease and/or death.

Immediately after the infection, *S. aureus* disappeared from the blood and rapidly disseminated in all the organs (64). In particular, the most infected organs were the kidneys, as illustrated in figure 8, which were therefore chosen as markers for systemic infection.
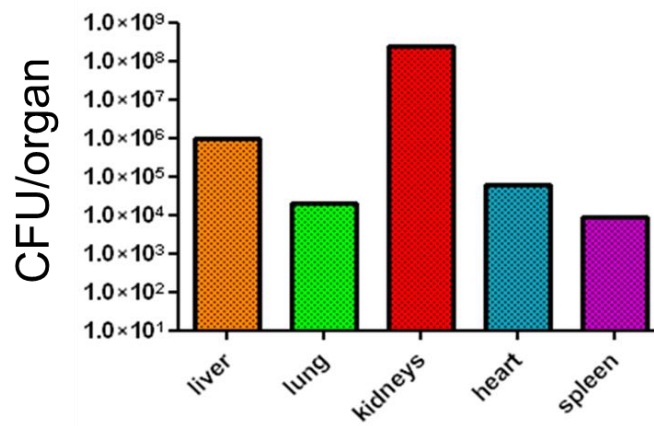
Figure 8. *Staphylococcus aureus* **intravenously injected in CD1 mice reached all organs.** CFU counts in organs 4 days after intravenous administration of about 1×10^7 CFU/mouse of *S. aureus* Newman strain. CFU were normalized among different organs reporting the total colonies counted in that organ.

Mice were intravenously infected with doses ranging from 1×10^7 to 1×10^4 CFU/mouse and followed up to 3 weeks post infection. Kidneys of infected animals were collected and knee joints washes were performed. In figure 9 we reported the results that we obtained. Mice treated with the dose of 1×10^7 showed evident signs of illness and, from four days after the infection, they started dying, while doses as low 1×10^5-1×10^4 resulted in poor or even absent infection. For these reasons a dose of 1×10^6 was chosen for our purposes since no animal died during this observation period and all of them resulted significantly infected both systemically and locally.
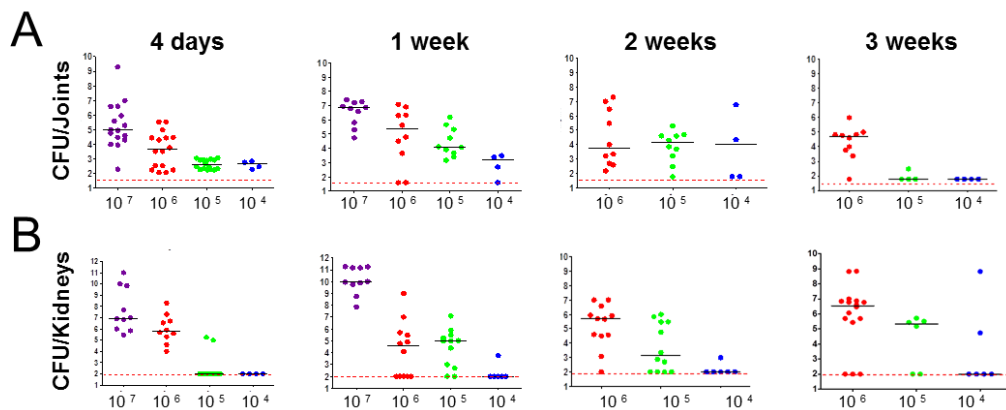
Figure 9. The dose of 1×10^6 CFU/mouse was used to establish a long lasting and reproducible model of arthrosynovitis in mice. A) CFU counts in knee joints washes of CD1 mice intravenously infected with *S. aureus* Newman strain. Animals were infected with different doses from 1×10^7 to 1×10^4 CFU/mouse and then sacrificed at day 4, and 1, 2 and 3 weeks after injection. Single dots represented single animals and different colors were used for the different doses. B) CFU counts in kidneys of mice infected i.v. with Newman strain. Doses ranging from 1×10^7 to 1×10^4 CFU/mouse were used and animals were sacrifice 4 days, 1, 2 and 3 weeks after injection. Single dots represented single animals and different colors were used for the different doses.

After this preliminary experiment, we inoculated animals with 10^6 CFUs and we followed the progression of *S. aureus* dissemination up to 90 days after the infection. Also in this case CFU counts in kidneys were used as marker of systemic infection and CFU counts in joint washes as marker of local infection in the knees joints. We additionally measured CFUs in the blood as a possible second

marker of systemic infection since it had been reported that during the chronicization of the pathology *S. aureus* could escape from the organs ad exploit the bloodstream for further spreading (64)

As reported in figure 10, the peak of the infection seemed to be reached between 1 and 2 weeks after the inoculum when CFUs recovered in joints and kidneys were maximal (fig.10 A-B). Starting from 1 month after infection, the CFUs started to decrease both in kidneys and in knee joints as the infection was being controlled by the host to a certain extent. On the other hand, CFUs in the blood seemed to increase during time reaching the highest level at the latest time point 90 days after infection (fig.10 C). Some animals actually died during the experiments not always showing evident signs of disease. In particular, 2 out of 24 died between day 15 and day 30 and 4 out of 18 died between day 30 and day 90.
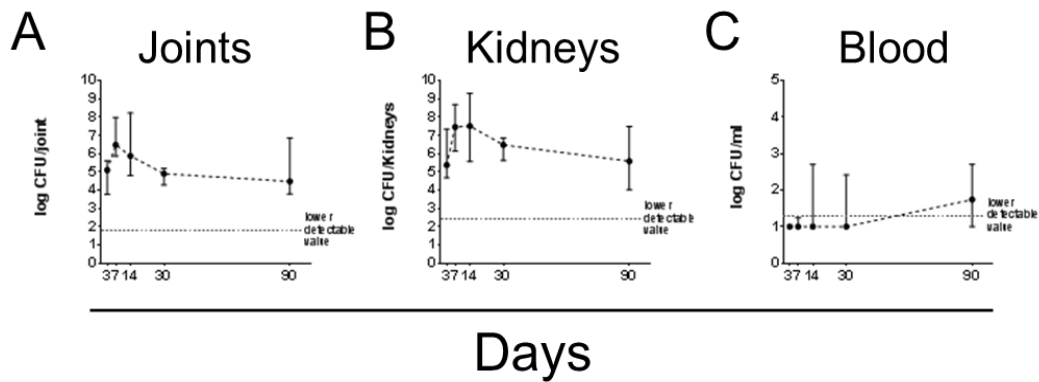
Figure 10. Bacteria could be detected up to 90 days after infection in knee joints, kidneys and blood. A-B-C) Logarithmic scale of bacterial titers in knee joint (A) kidneys (B) and blood (C) were determined at indicated time points. Each point represents the median and the bars reported the interquartile range.

To better understand whether the infection was being controlled or was becoming chronic, we performed H&E staining of slices from knee joints of infected mice up to 90 days post intravenous infection. In figure 11 we reported the results of our observations expressed in terms of severity and chronicization (age-grade) of all samples analyzed. These analyses demonstrated that after intravenous infection with *S. aureus*, mice developed arthrosynovitis and osteomyelitis and that both an acute (7-14 days) and a sub-acute/chronic (90 days) phase could be clearly detected.

normal	0
mild	1
moderate	2
severe	3
very severe	4
Extremely severe	5

normal	0
iperacute	1
acute	2
subacute	3
chronic	4
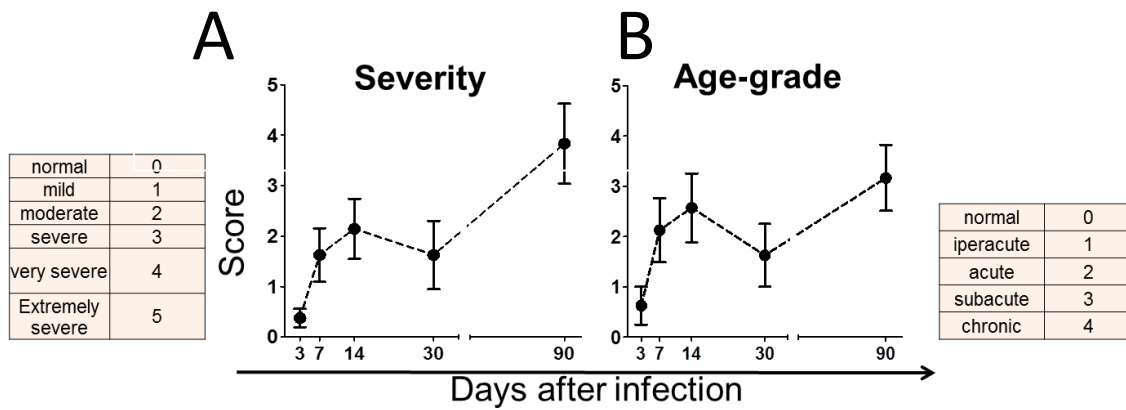
Figure 11. Intravenous infection with *S. aureus* resulted in an initial acute phase that finally chronicized. A-B) Severity (A) and age grade (B) of arthrosynovitis and osteomyelitis during the time. A specific score (indicated in the tables) was assigned for severity and age grade of the disease for each knee slides analyzed at each time point. Six mice for time point were analyzed and medians plus interquartile range were reported.

2.2_2 Serological analysis

The humoral response during the time both *in* situ and systemically was also analyzed. IgM and IgG against alpha-hemolysin (Hla), one of the most important and highly immunogenic virulence factors of *S. aureus*, were titrated both in sera and in the joint washes of infected mice at each time point as marker of infection progression.

Anti-Hla IgM peaked seven days after the bacterial injection both in the knee joints and in the serum, while IgG level reached the maximum level at 14 and 30 days after inocula in joint and serum respectively, decreasing then in knee washes along with CFU

decrease, while remaining almost stable during the time in the sera of infected animals as expected (fig.12).
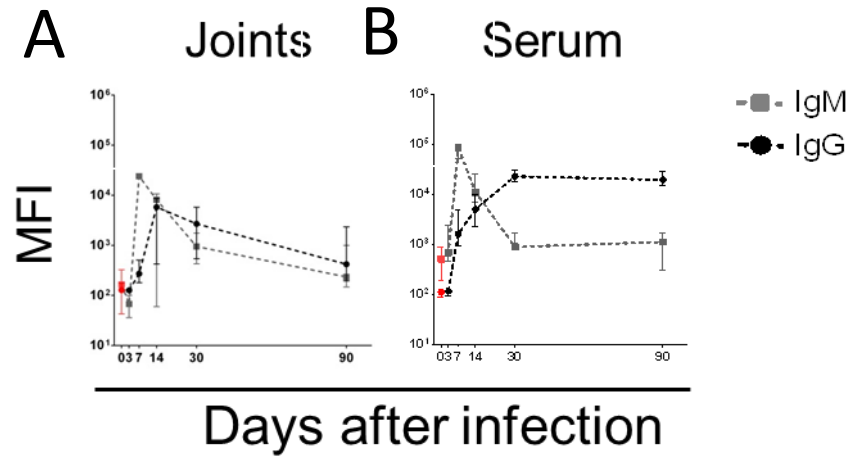
Figure 12. IgM and IgG could be detected both in the sera and in the knee lavages of infected animals. A) Hla IgG (black line) and IgM (grey line) curves in knee joint washes of infected animals from day 0, in red and pink, respectively through day 90. Medians and interquartile ranges were reported. B) Hla IgG (black line) and IgM (grey line) curves in sera of infected animals from day 0 (pre-infection time) through day 90. Medians and interquartile ranges were reported.

As cytokine secretion can be considered a reliable indicator of immune activation, we also assessed cytokine levels at different time points after infection. In order to understand if the local inflammatory response was specific and if differences existed with the systemic response, we measured cytokine levels both in the serum and directly *in situ.* The cytokines analyzed were IL-1α, IL-1β, IL2, IL-3, IL-4, IL-5, IL-6, IL-9, IL-10, IL-12 (p40), IL-12 (p70), IL-13, IL-17,

eotaxin, G-CSF, GM-CSF, IFNγ, KC, MCP-1, MIP-1α, MIP-1β, RANTES and TNF-α. In the knee joints (fig.13) all the cytokines that increased (IL-1α, IL-1β, IL-6, IL-10, IL-12 (p40), IL-17, eotaxin, G-CSF, GM-CSF, IFNγ, KC, MCP-1, MIP-1α, MIP-1β, RANTES) in comparison with time 0 (not infected animals) showed a profile of expression that somehow correlated with the observed trend of CFU number variation during infection (fig. 10A). Interestingly, IL-9 and IL-13 were the only 2 cytokines that displayed an opposite trend, decreasing during the time as compared to controls. Finally some of them did not significantly change during the time (IL-2, IL-3, IL-4, IL-5, IL 10, IL12p70 and TNF-α).
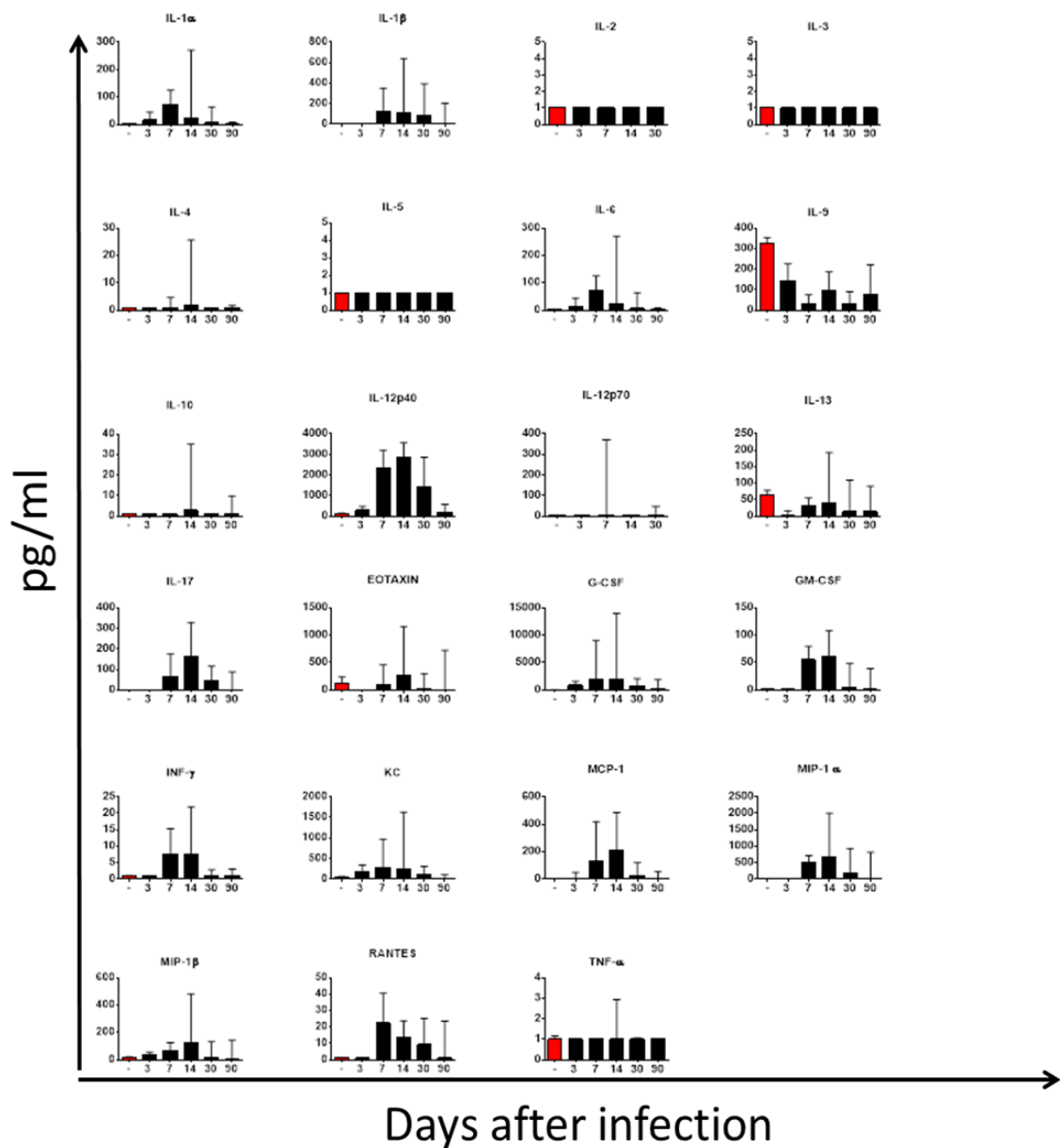
Figure 13. Cytokines profile in knee joint washes of infected animals during the time. A panel of 23 cytokines was analyzed in knee joint washes. In red data obtained with negative controls (not infected animals) are reported. In each graph the median and interquartile ranges of one cytokine is reported in pg/ml. The name of the cytokine analyzed is reported above each graph.

The situation in the serum (fig. 14) was different and more complicated: some cytokines did not change during the time (IL-1α, IL-2, IL-3, IL-4, IL-9 and RANTES); others (IL-6, eotaxin and KC) were secreted immediately after the infection (3 days) and then decreased during the time, or showed a kind of bimodal behavior (IL-1β, IFNγ); others increased rapidly remaining then stable (IL-5, IL-10, IL-12(p40), IL-12(p70), IL-13, IL-17, G-CSF, GM-CSF, MCP-1, MIP-1β, TNF-α). MIP-1α seemed to be secreted only at the latest time point.
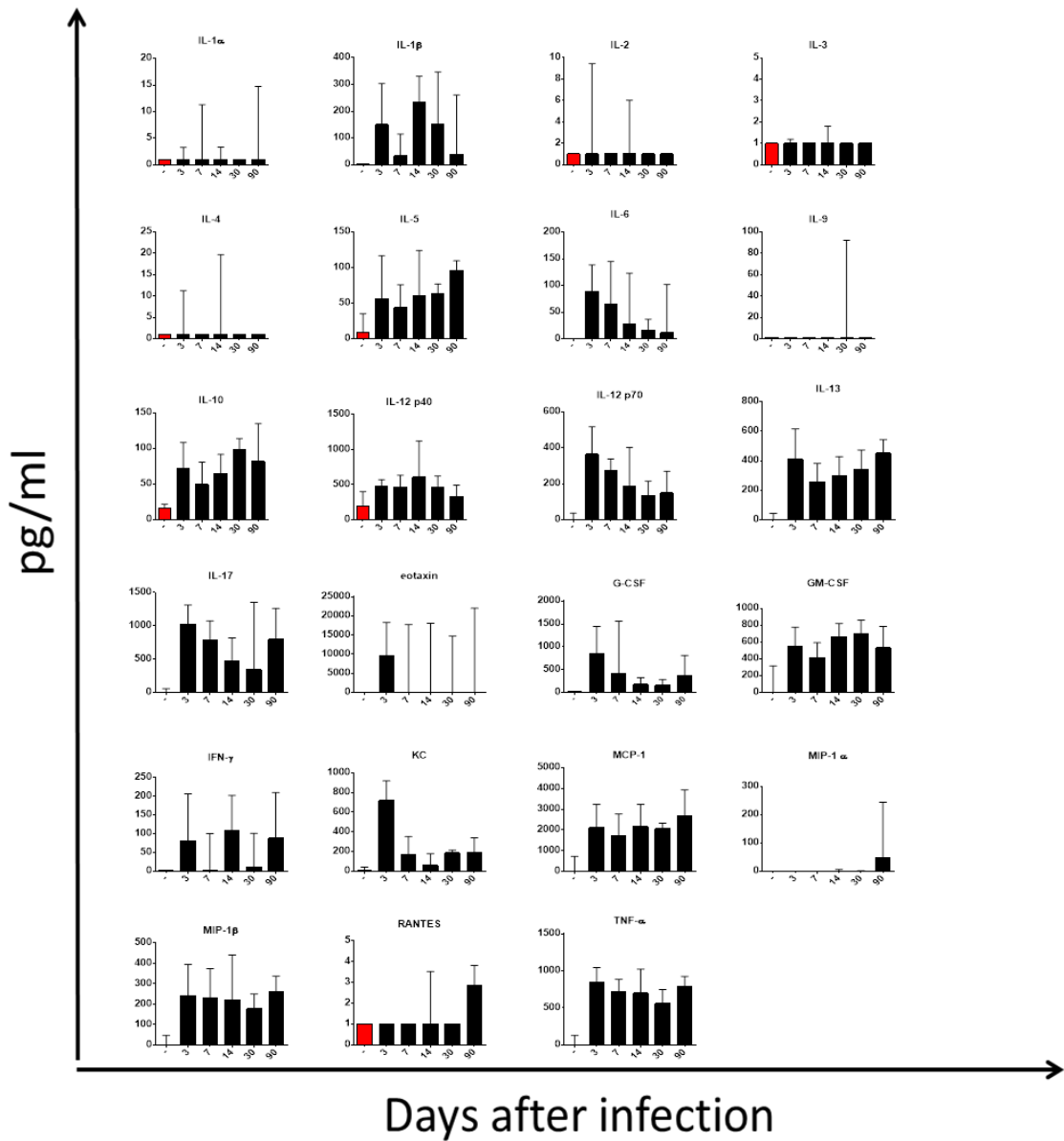
Figure 14. Cytokines profile in sera of infected animals during the time. A panel of 23 cytokines was analyzed in sera of infected mice. In red data obtained with negative controls (not infected animals) are reported. In each graph the median and interquartile ranges of one cytokine is reported in pg/ml. The name of the cytokine analyzed is reported above the single graphs.

Some of the cytokines found in the knee joint washes well correlated with the CFU recovered in that site at different time points. In particular, as reported in figure 15, for most of them this correlation could be detected 14 days after infection (IL-6, IL-12(p40), IL-13, IL-17, G-CSF, KC, MCP-1, MIP-1β, RANTES), while for IL-12(p40) and MIP-1α a good correlation was found at days 30 and 90 post infection respectively.
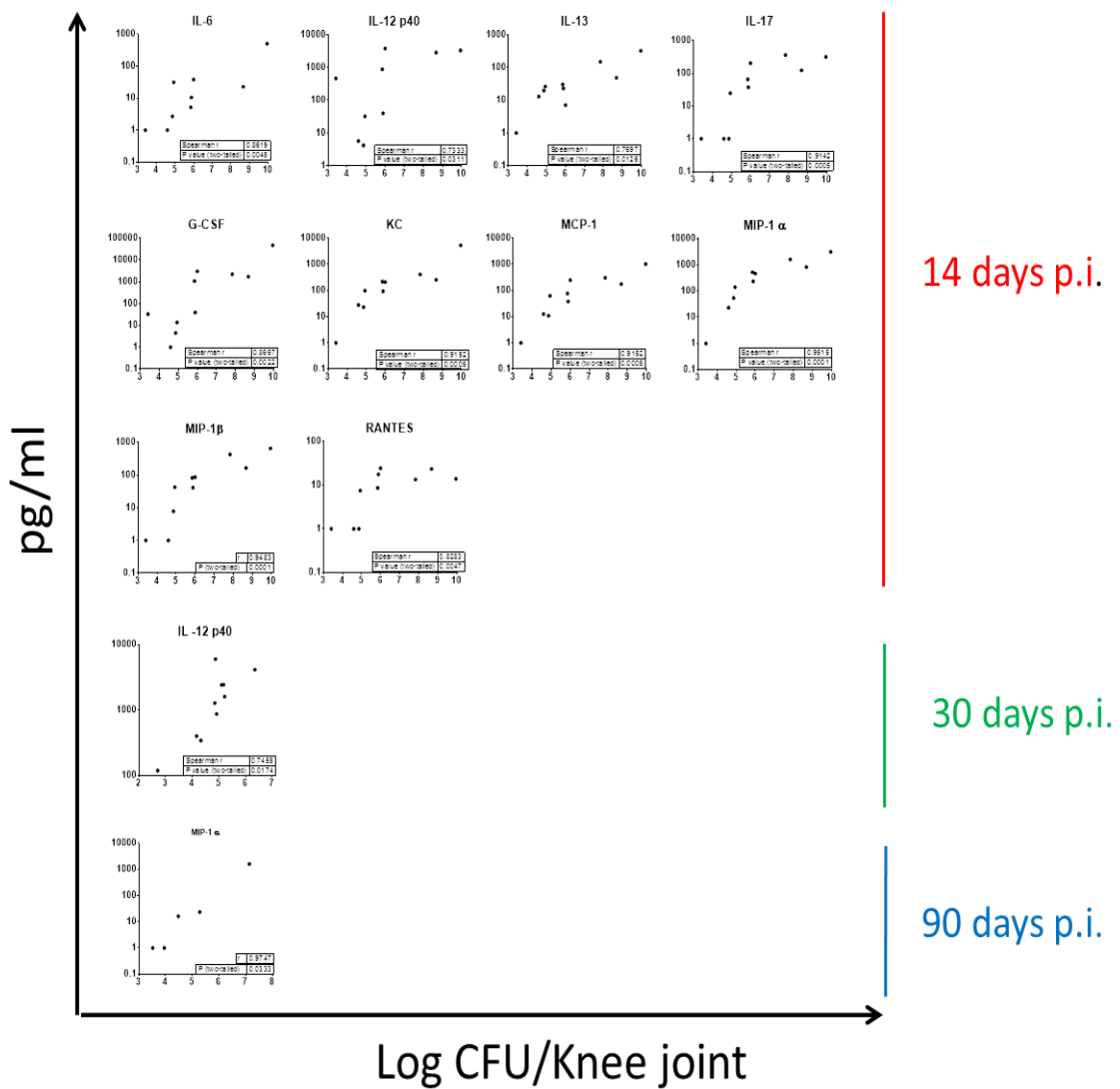
Figure 15. Cytokines which correlate with CFU number in knee joints.

A correlation analysis between cytokines levels and CFUs recovered in the knee joint of single animals was performed. In the panel only significant correlations are reported together with Pearson R index and statistical analysis for each situation. Single dots represent single animals. Each graph reports the name of the respective cytokine and, on the right, the different time points are reported.

2.2_3 Cellular analysis

We also analyzed at each time point the immune cell populations recruited in the knee joint space and present in the blood of infected animals. First we wanted to understand if and how intravenous infection with *S. aureus* could affect the immune cell composition in knee joint washes. In figure 16 we reported the number of live cells recruited in joint washes 1 week after infection with *S. aureus* Newman strain and we compared this number with that obtained from cells recovered in mice mock-infected with PBS alone. As shown in the picture, as early as 1 week post infection the immune cells counted in the knee joints of infected animals were almost 100 fold higher than those recovered in uninfected mice.
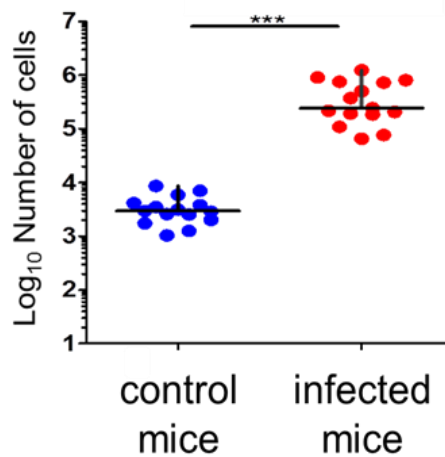
Figure 16. The number of live cells in knee joint washes increased after *S. aureus* infection. Live cells recovered in knee joint washes of control mice injected with 100 µl of PBS (blue dots) and infected mice injected with the same volume of $2x10^6$ *S. aureus* Newman strain (red dots). Logarithmic scale was used to graph these data and medians line are aso reported.

The next step was staining those cells with specific antibodies directed against different cellular markers to better characterize the multiple cell populations. Through the gating strategy reported below, we were able to identify neutrophils, macrophages (only in knee joint washes), monocytes, dendritic cells, eosinophils (only in blood), B cells, CD4+ and CD8+ T cells, NK cells.
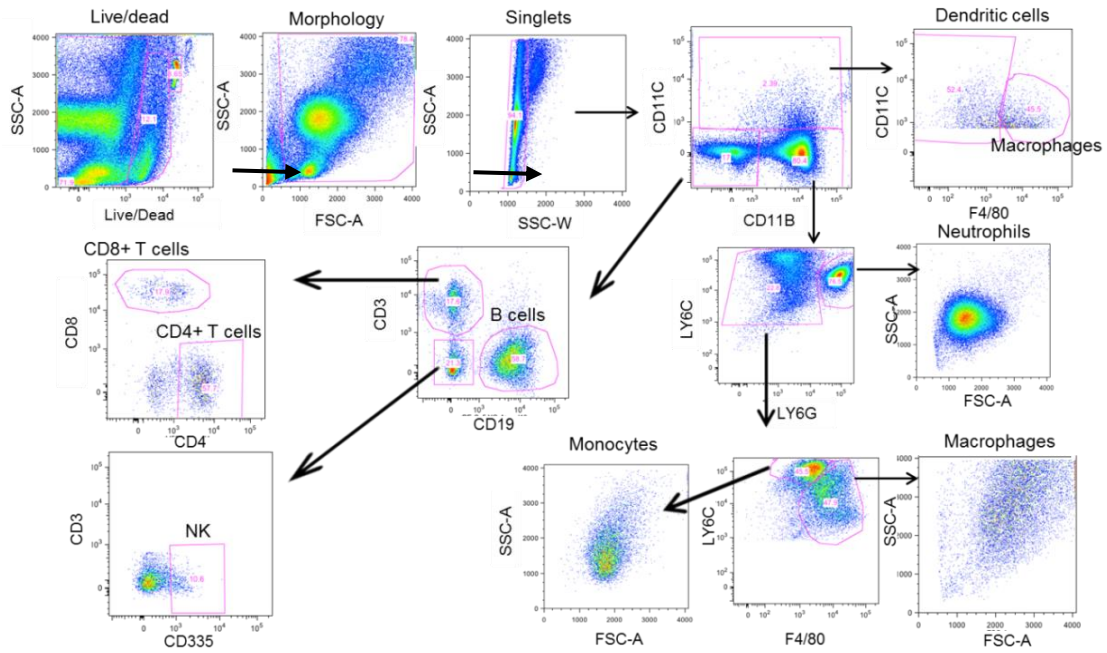
Figure 17. Gating strategy used for the identification of immune cells in knee joint washes and blood. Cellular composition of knee joint washes and blood was analyzed using the gating strategy reported above. Gate edges were underlined in pink and the name of the single cell subsets identified using that strategy was reported above the panel or above the single gate. X and Y axes reported the physical or immunological parameter used for preparing each specific panel. Black arrows indicated the analysis sequence.

Locally, in the knee joints (fig. 18), cells belonging to the myeloid lineage increased starting from three days after the infection with an evident peak at 1 - 2 weeks post inoculum, which recalls the observed bacterial profile described in figure 10A. Neutrophils were the most abundant population increasing up to 1000 fold as

compared to the basal situation, but also monocytes and macrophages showed a sharp increase (10-50 fold). A similar situation, although less evident, was observed when myeloid cells were stained and counted in the blood. In this case a decrement in eosinophils, especially immediately after infection, was observed. Different the behavior of lymphoid cells *in situ* and systemically. Indeed, while lymphoid cells decreased in the blood starting 3 days after the injection with *S. aureus*, they increased in the joints. Noteworthy, this was true for all the lineages but not for B cells that significantly decreased in number also in the joints. During the chronic phase the cellular composition both in blood and in the knee joint came back to the baseline level.
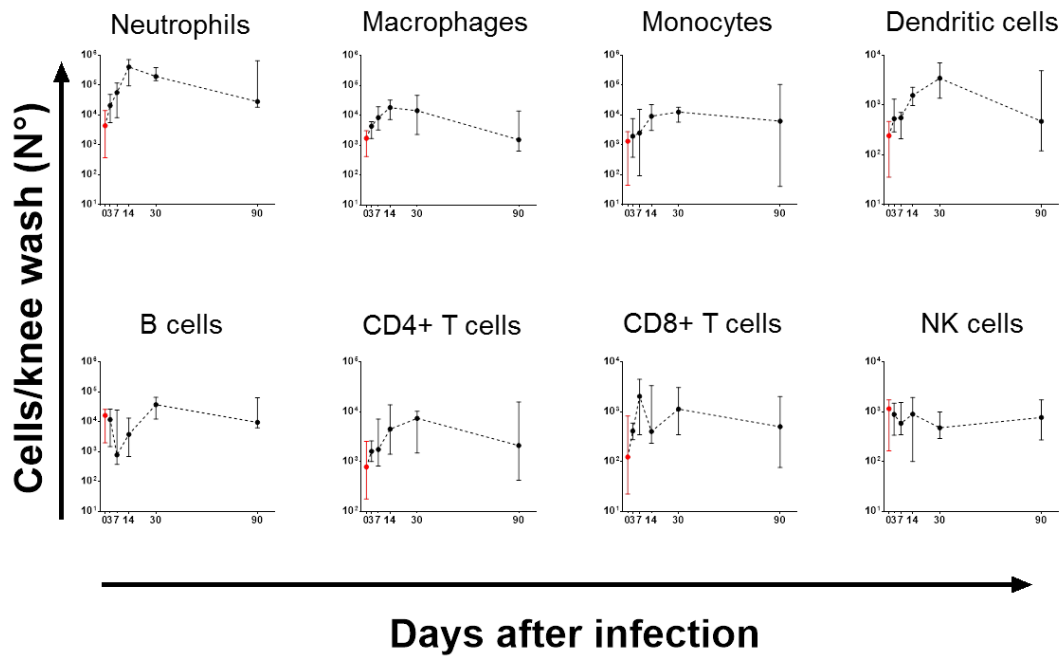
Figure 18. Immune cell analysis of mouse knee joint washes. Absolute cell numbers of immune cells identified in knee joint washes of *S. aureus* infected animals and control mice. Starting from time 0 (control animals in red) and through all the observation period (90 days, black line and dots) animals were sacrificed at established time points and immune cells recruited in knee joints were collected and stained. In the graphs, single subset populations are shown as indicted in the titles.
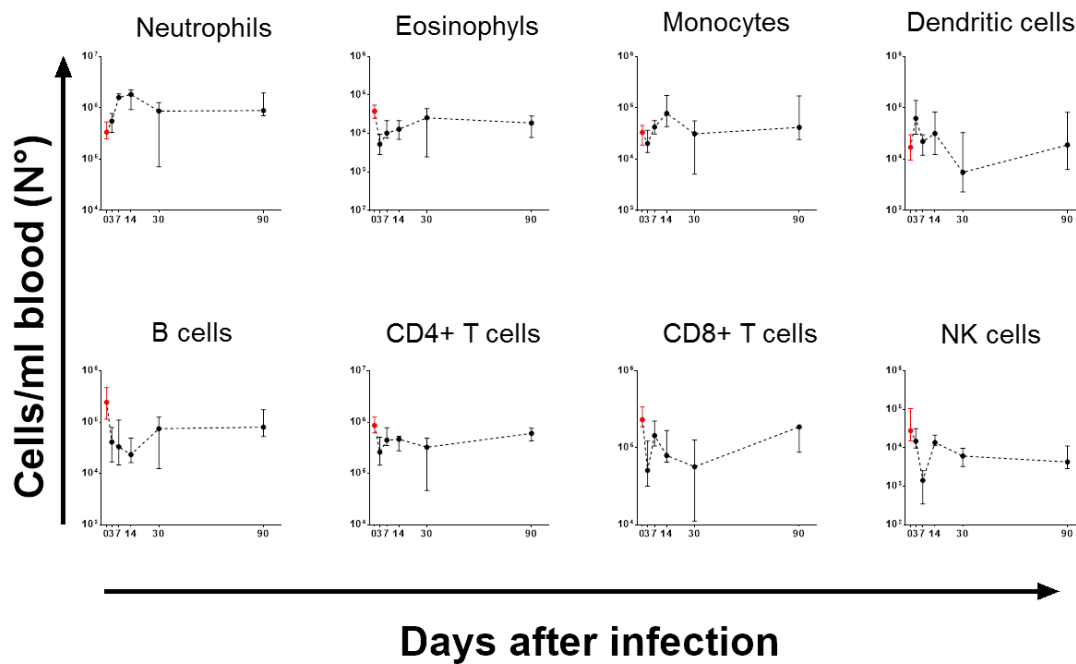
Figure 19. Immune cell analysis of mouse blood. Absolute cell number of immune cells per ml of blood identified in *S. aureus* infected animals and control mice. Starting from time 0 (control animals in red) throughout all the observation period (90 days, black line and dots) animals were sacrificed at established time points and immune cells in the blood were collected and stained. In the graphs, single subset populations are shown as indicted in each title.

2.3 The acute arthrosynovitis model can be used to test therapeutic and preventive treatments against *S. aureus* infections

2.3_1 Ampicillin treatment reduced bacterial load in kidneys but was not efficacious in killing *S. aureus* in knee joints

In humans antibiotics are the first and most used treatment for *S. aureus* septic arthritis and osteomyelitis (65). Nevertheless, sometimes they are not able to eradicate bacteria from these sites because of the low vascularization of bones and joints and of the increase of *S. aureus* antibiotic resistant forms. In order to investigate whether a classical antibiotic treatment would be able to reduce bacterial burden in our model, mice infected i.v. with about $2X10^6$ bacteria of the *S. aureus* Newman strain were treated i.p. with 100µg/g weight of ampicillin 24 and 48 hours after infection, as reported in literature (66). Five days later they were sacrificed, kidneys were collected and knee joint washes were performed.

Interestingly, a significant reduction in CFU counts was observed in kidneys (fig. 20A), indicating that the antibiotic treatment had some positive effect on the containment of the systemic infection. On the contrary, a CFUs reduction in knee joints (fig. 20B) was not

observed, which could be expected on the basis of the reported difficulties to successfully treat with antibiotics such localized infections.

When the cell composition in knee joint washes was analyzed no substantial differences were observed, with the exception of B cells, which appeared to be more abundant in the animals treated with ampicillin (fig. 20C).
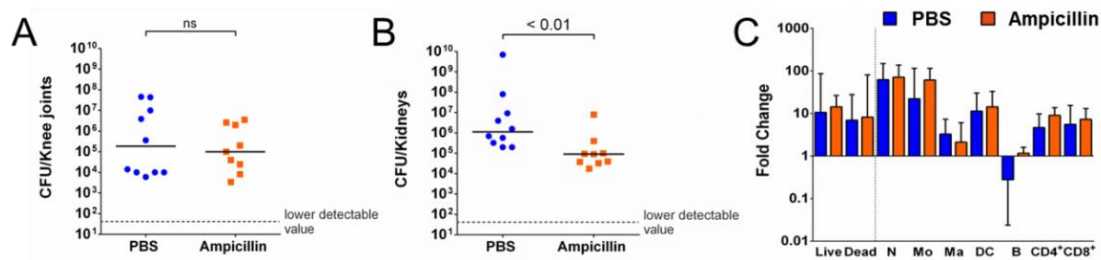
Figure 20. Mice treated with ampicillin after infection with *S. aureus* Newman strain showed reduced bacterial load in kidneys but not in knee joints. A) CFU counts in knee joint washes of mice intravenously infected with *S. aureus* Newman strain and treated intraperitoneally twice with ampicillin 100 μg/g of body weight 7 days after inoculum. Each dot represented data from one single animal and black lines showed median values. The dotted grey line stated the lower detectable value. B) CFU counts in kidneys of mice intraperitoneally treated with ampicillin after being infected with *S. aureus* Newman at the dose of 2×10^6 CFU/mouse. Each dot represented one single animal and black lines showed median values. The dotted grey line stated the lower detectable value. C) Immune cell recruitment in knee joint washes of mice infected with *S. aureus*, treated twice with ampicillin and sacrificed 7 days after bacterial inoculum. Fold change in respect to the normal situation (median of naïve mice for each cellular subset) was plotted, medians and interquartile range were shown. N= Neutrophils, Mo= Monocytes, Ma= Macrophages, DC= Dendritic cells, B= B cells, CD4+= CD4+ T cells, CD8+ =CD8+ T cells. Statistical analysis was performed with a Mann-Whitney t test in all the cases and only statistically significant differences were reported.

2.3_2 The Novartis vaccine proposed against *S. aureus* infections reduced bacterial burden in joints of infected mice

The described model of acute arthrosynovitis in mice was then used to test the Novartis proposed vaccine against *S. aureus* mediated infections. Novartis vaccine is a combination (called "combo") of 4 protective antigens, a detoxified form of alfa-hemolysin (HlaH35L) where histidine 35 was mutated with a leucine, the fusion protein EsxA-B that consisting of the 2 extracellular secretion system proteins A and B both involved in infection persistence (61), the highly conserved ferric-hydroxamate uptake D2 (FhuD2) (58) protein, important in the early stages of infection and Sur 2, a surface lipoprotein highly conserved and still poorly characterized. Different groups of mice received two immunizations with a two-week interval either with the combo vaccine adjuvanted with aluminum hydroxide (alum) or the adjuvant alone as negative control. Ten days after, the animals were infected with about $2X10^6$ CFU/mouse intravenously, they were sacrificed 7 days after and kidneys, blood, serum were collected together with knee joint washes to perform microbiological and immunological analysis.

As shown in figures 21A and 21B, immunization with the protein combination resulted in a significantly lower bacterial burden both in

the knee joints (A) and in the kidneys (B), suggesting that, in this model, the efficacy of a preventive vaccine treatment may be more efficacious than a classical therapeutic approach in reducing *S. aureus* mediated infection in joints.
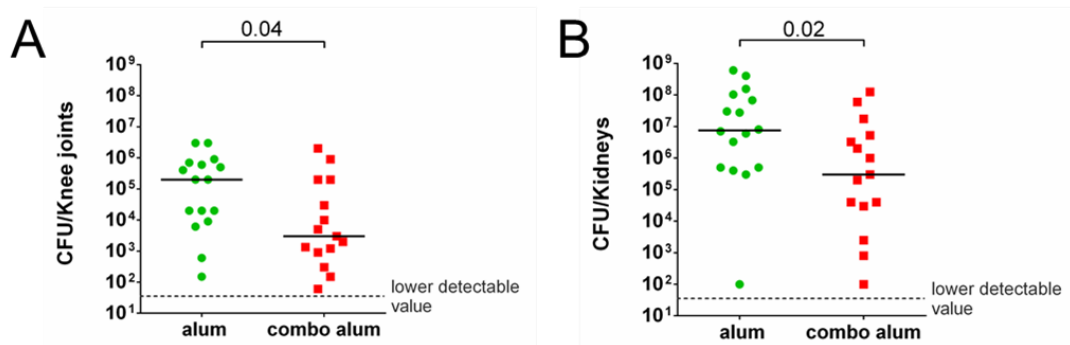
Figure 21. Mice immunized with the *S. aureus* combo vaccine resulted protected against a subsequent systemic infection with *S. aureus* Newman strain. A) CFU counts in knee joint washes of mice immunized and intravenously infected with *S. aureus* Newman strain 7 days after inoculum. Each dot reports the data from a single animal and black lines indicate the median values. The dotted grey line states the lower detectable value. B) CFU counts in kidneys of mice infected with *S. aureus* sacrificed 7 days later on. Each dot is referred to a single animal and black lines show median values. The dotted grey line states the lower detectable value. In both the cases, statistical analyses were performed with a Mann-Whitney t test.

Further analyses were then performed in the attempt to understand the possible mechanism(s) of action of the vaccine. To this purpose, we analyzed both the humoral and the cellular immune components.

First we measured antibody titres against each single antigen of the vaccine in the knee joint washes. In figure 22A IgG titres against all the antigens are reported, demonstrating that all of them induced seroconversion in immunized animals and that measurable antibody levels could be detected in the knee joints.

Moreover, immune cells were analyzed comparing the results obtained for the vaccinated animals to those obtained for the negative controls. Fewer dead cells were found in knee joint washes of combo-immunized mice and, even if the number of total cells recovered was more or less the same in both the samples, the number of neutrophils recruited was lower in the immunized group indicating the lower state of general inflammation (fig.22B). Interestingly, B cells were preserved in knee joints after immunization with protein combo as if the vaccination could increase the number of cells recruited and/or shield them from *S. aureus* mediated toxicity (fig. 22B).

Cytokine levels were also measured in this site. Even if none of the analyzed mediators significantly changed between the 2 groups, it was interesting to note that almost all the pro-inflammatory cytokines (like IL-1α, IL-1β, and G-CSF) were a little less in knee joint washes of combo immunized animals in respect to mocked immunized mice (fig. 22C), confirming the observation already done of a general lower state of inflammation of treated animals.
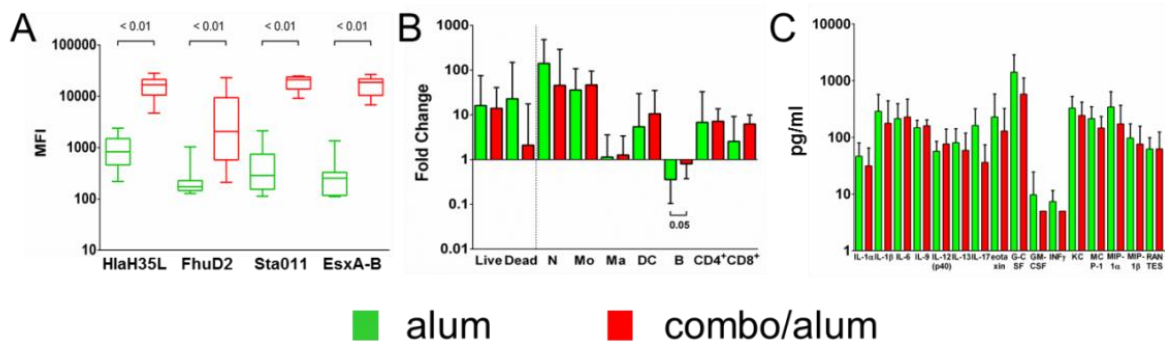
Figure 22. IgG titres, immune cells recruitment and cytokines analysis of immunized mice. A) IgG titres of combo antigens from knee joint washes of mice immunized with alum or combo/alum and infected with *S. aureus* Newman strain. Mean Fluorescence Intensity (MFI) was used as titer and box-whiskers analysis (median plus 25 and 75 percentile) of row data was reported. Statistical analysis was performed with a Mann-Whitney t test. B) Immune cell recruitment in knee joint washes of mice immunized and infected with *S. aureus* 7 days after infection. Fold change in respect to the basal situation (median of naïve mice for each cellular subset) was plotted, medians and interquartile range were reported. N= Neutrophils, Mo= Monocytes, Ma= Macrophages, DC= Dendritic cells, B= B cells, CD4+= CD4+ T cells, CD8+ =CD8+ T cells. Statistical analysis was performed with a Mann-Whitney t test. Only statistically significant differences were reported. C) Cytokine analysis of knee joint washes from mice immunized with alum or combo/alum and infected with *S. aureus* Newman strain. Data were reported in pg/ml and only the cytokines from a panel of 23 mediators analyzed which were measurable were shown. Medians and interquartile range were reported and statistical analysis was performed with a Mann-Whitney t test. Only statistically significant differences were shown.

3 Discussion

In the present work we set a new, long lasting and reproducible mouse model of *S. aureus* mediated arthrosynovitis-osteomyelitis that allowed us to unravel the host immune response during these pathologies. Using this model we were also able to demonstrate that the Novartis proposed Vaccine against staphylococcal infections overcame the activity of a commercial antibiotic in reducing bacterial load in knee joints. High IgG titres against all the vaccine components were found in knee joint washes of vaccinated animals one week after infection with *S. aureus* Newman strain. Moreover, vaccination seemed to preserve the immune cells recruited in joints after infection by bacteria-mediated killing and this was particularly clear for B cells. Finally, a lower degree of general inflammation was observed in knee joints of vaccinated animals as compared to the controls that reflected a lower recruitment of neutrophils *in situ*. We can conclude that this vaccine could become a powerful tool for preventing *S. aureus*-mediated arthrosynovitis and osteomyelitis in humans, pathologies that still have often poor outcomes.

Septic arthrosynovitis and osteomyelitis are severe and painful joints and bones diseases often associated with treatment failure and poor prognosis. Most of these pathologies are due to *Staphylococcus aureus* that is also responsible for the ones with the highest complications (67).

Since the pathophysiology of these diseases is not completely understood, the use of animal models has proven invaluable for studying them as well as for testing the efficacy of experimental preventive and therapeutic treatments (68). To mimic the human disease as closely as possible, several features of the host bacterium relationship should be clarified. During the past decades, the use of experimental models of staphylococcal infections was useful to understand the involvement of several bacterial virulence factors as well as the host response to the bacterial infection. Dogs, rabbits, rats, chickens, and mice (69,70,71,72,73) have been used to develop *Staphylococcus aureus* model of arthrosynovitis and osteomyelitis, but it is believed that the mouse model is optimal because of the resemblances between the murine and the human immune and inflammatory systems.

Nevertheless, the existing animal models generally study osteomyelitis and arthritis like two different diseases but since these pathologies often coexist in humans, they do not completely reflect the full scenario of the natural disease. Moreover, most of them focus only on the acute phase of the disease while the chronic phase, which occurs later on during the infection, is often the most debilitating one (74,75). Recently Horst et al. developed a novel hematogenous murine model of acute and chronic osteomyelitis, but the immune response induced has not been analyzed neither locally nor systemically (72).

Based on this background, we thought it would be important to have a consistent model of osteomyelitis and arthritis established in mice after infection with *S. aureus*, which would allow to study both the acute and chronic phases, dissecting the humoral and cellular host immune response locally and systemically, and to evaluate the efficacy of therapeutic and preventive tools.

An important issue was how the staphylococci spread through the body to reach the joints. The most common routes of infection for both septic arthritis and osteomyelitis in humans are the haematogenous, the contiguous, or the direct ones (13, 14, 15, 16, 17), but it was clearly shown that most of bacterial joint infections in humans are caused by bacteria which spread hematogenously (18).

Thus we decided that intravenous (i.v.) inoculation of bacteria mimicking the hematogenous route of infection would be the optimal delivery route for the animal model that we wanted to set up. Indeed after inoculum, bacteria are required to adapt to the environment within the host, to survive bactericidal components in the blood, disseminate to synovial tissue and penetrate various structures to reach the joint space (69) being in this way really similar to what happens during natural infections in humans.

We reported in figure 5 using the In Vivo Imaging System (IVIS$^{®}$) that *S. aureus* showed a particular tropism for bones and joints

considering its ability to quickly and long lastingly colonize these tissues. This was somehow expected since *S. aureus* expresses several receptors (adhesins) specific for bone matrix components such as fibronectin (76), collagen (77) and bone sialoprotein (78). Once reached the joints *S. aureus* was able to cause both arthrosynovitis and osteomyelitis and the infection lasted for months progressing to a chronic phase (figures 7, 10A and 11). Interestingly, only combining histopathological and microbiological analysis of both the *in situ* and the systemic situation we were able to clearly identify an acute and a chronic phase of arthrosynovitis and osteomyelitis. On the one hand CFU decrease in the knee joints and kidneys seemed to push toward the resolution of the pathology, but on the other hand the rise of CFU in the blood and, in particular, the increase in age grade and severity of histopathological analysis of knee joints showed a completely different scenario. The acute phase was therefore characterized by a high bacterial burden in joints and kidneys, but medium level of severity of the lesions in the knee joints, while when the infection became chronic, CFU numbers decreased, as the host immune system was able to control bacteria, but the severity of the lesions dramatically increased with destruction and deformation of the bone architecture, and bacteria used again the blood as vehicle for further dissemination. Taken together, these data allowed us in defining the two distinct phases of infections, an acute

phase that picks from 7 to 14 days after inoculum, and a chronic phase, that could be clearly seen at the latest time point.

Like in humans, the acute phase was shown to be highly symptomatic and was characterized by a particularly active immune response.

Interestingly, the host immune response, both humoral and cellular, seemed to be quite different between blood and knee joints indicating that a specific immune response is built up against this pathogen *in situ*. While in the blood the situation was quite complicated probably representing a multi-organ infection, during this phase all the pro-inflammatory cytokines (like IL-1β, IL-6 and IL12p40) peaked in the knee joints between 7 and 14 days after infection, reflecting the profile observed for CFU counts and allowing the recruitment of the cellular components of the host immune response. Moreover, a good correlation between some of the cytokines we analyzed and CFU counts in knee joints was observed (figure 15). This important finding could pave the way for using new potential biomarkers for humans, that could be not only useful in the specific diagnosis of the diseases, but above all to define the degree of severity and the maturation of disease, helping to figure out the possible prognosis and to give the most proper and accurate care for a patient.

As expected, IgM and IgG levels rose significantly early during the acute phase indicating that a strong adaptive immune response was mounted against the pathogen really soon and that the inflammation

state of the joints was useful in allowing the diffusion of antibodies and the recruitment of plasmacells *in situ*. But inflammation means also cellular recruitment. We therefore approached the cellular analysis both in the knee joints and in the blood using, in our knowledge for the first time in these models, a flow cytometer analysis with a specific staining for different immune cells. This approach allowed us analyzing almost all the possible immune cells recruited in this site at the same time.

Both myeloid and lymphoid cells were rapidly and strongly recruited *in situ*. Monocytes and macrophages increased between 10 and 20 fold starting immediately after infection. These cells play an important role in controlling initial stages of infection not only directly through the phagocytosis of the bacteria, but also producing chemoattractant molecules for neutrophils recruitment. Their role in the early stages of infection is in any case controversial. Verdrengh et al. (79) indeed studied the role of these cells in staphylococcal arthritis using monocytopenic mice. During the time these mice exhibited a significantly less severe arthritis than the control animals and this was accompanied by decreased serum levels of the proinflammatory cytokines TNFα and IL-6. In contrast, infection-triggered mortality was increased in the monocytopenic mice as compared with the control animals. Notably, the monocytopenic mice exhibited elevated bacterial burden in the blood and kidneys. This study indicated a dual role of mononuclear phagocytes in the pathogenesis of *S. aureus*-

induced infection. On the one hand, absence of macrophages led to a favorable outcome concerning the severity of arthritic lesions, but on the other hand the direct and indirect clearance of bacteria mediated by monocytes/macrophages was decreased, resulting in poor survival. Neutrophils were actually the population which showed the highest increment among all the cells changing almost 1000 fold as compared to not infected mice. This increment was evident in the blood too, even if less impressive, probably suggesting a greater production due to an increased demand from other tissues and organs. It is not strange to see that neutrophils were strongly recruited in the knee joints immediately after infection peaking at 14 days, since it had been already demonstrated that they played an essential role in controlling bacterial spreading in these kinds of infections. Indeed mice depleted of these cells died in a few days after infection with *S. aureus* and showed more severe signs of arthritis, increased bacterial burden in blood and kidneys and exhibited increased levels of the proinflammatory cytokines TNFα, IL-6, and INFγ, reflecting the severity of their disease (80,81).

The role of T cells in arthrosynovitis and osteomyelitis was already reported by Abdelnour et al. (82) who showed using a immune-histochemical approach an increase of these cell populations in the joints between 3 and 14 days after the bacterial inoculum. We confirmed their findings but our approach was certainly more suitable for studies where a large number of animals and multiple analyses

were required. During the first days after infection circulating lymphoid cells left the blood spreading into tissues where they were recruited by the presence of infective agents. Interestingly, while CD4+ and CD8+ cells incremented in the knee joints from day 3 to day 14 confirming our hypothesis, this was not true for B cells whose number suddenly decreased coming back to basal level only between day 14 and day 30.

One possible explanation for this behavior is the production by *S. aureus* of protein A (Spa). In recent studies, it was shown that SpA has the properties of a B cell superantigen by virtue of interactions with a large supraclonal B cell set via high affinity framework-mediated interactions with soluble and cell-associated B cell receptors (BCR, 83). Moreover, other studies demonstrated that a domain of SpA forms a complex with human Fab via a conformational surface on BCR (84) and that this target is conserved among amphibian, avian, and mammalian species (85).

SpA toxic activity in vivo was already demonstrated by Goodyear et al. who injected in mice purified protein A and then followed the fate of peripheral B cells expressing BCRs with VH regions capable of binding SpA. They observed a rapid down-regulation of BCRs and the coreceptors CD19 and CD21, the induction of an activation phenotype, and limited rounds of proliferation. Apoptosis followed through a process heralded by the dissipation of mitochondrial

membrane potential, the induction of the caspase pathway, and DNA fragmentation (86). This apoptotic collapse is of course a key mechanism that suppresses adaptive immune responses during staphylococcal infection playing an essential role for *S. aureus* escaping of host immune system. In our knowledge we reported for the first time that *S. aureus* is able to kill B cells during an infection in a mouse model even if we cannot exclude that other bacterial proteins could be, together with protein A, in part responsible for this phenomenon. Nevertheless *S. aureus* could also reduce B cells in situ through indirect mechanisms, such as inhibiting host factors that recruit those cells directly in the sites where they are requested. Further investigations are required to unravel these open questions and to better explain the phenomenon we reported here.

The chronic phase was characterized by a general lower inflammation state in the knee joints as compared to the acute one, even if the severity of the lesions significantly increased. The cytokines profile *in situ* came back to basal level trailing behind also the number of cells. The lower inflammation was also highlighted by the decrease in antibody titres as if the remained *S. aureus* colonies could hide themselves to the host immune system. In fact Horst et al. demonstrated that *S. aureus* could form microcolonies within the nonmineralized collagen matrix or locate intracellularly within neutrophils (72). In the blood there seemed to be a restoring of the normal situation regarding the cell populations, but the cytokines

revealed the presence of a more complicated situation. Indeed, while some pro-inflammatory cytokines remained high throughout all the observation time (TNFα, GM-CSF, MIP-1β) showing a permanent state of inflammation, some others clearly declined during the last time points (IL-6, IL-1β, KC). This behavior could probably be partially explained by the presence of high level of anti-inflammatory cytokines secreted to control the activity of the inflammatory ones.

The model of *S. aureus* mediated arthrosynovitis and osteomyelitis we proposed is suitable for testing both preventive and therapeutic tools against this pathogen. Correlates of protection could also be found using such approach that will be useful for further development of vaccines and new antibiotics.

The proposed Novartis vaccine against *S. aureus*-mediated infections that we tested in this study demonstrated not only to be protective against this pathogen, but also to be more effective than an ampicillin treatment in reducing CFU infiltration in knee joints. As reported elsewhere (14) antibiotics even if effective in eradicate bacteria in multiple organs and tissues, often fail when pathogens reach joints and bones, probably because of the particular nature of these tissues (i.e. poor blood supply). For this reason, an effective vaccine against *S. aureus* joints and bones pathologies is of great interest. When mice were immunized with the *S. aureus* combo vaccine adjuvanted with alum phosphate, a reduction in CFU counts

both in kidneys and knee joints was observed. Similar results could be also obtained in kidneys with two injection of ampicillin, but this antibiotic was completely inefficacious against bacteria in knee joints. High antibodies titres against all the components of the protein combo could be detected in the knee joints lavages and this could partially explain the efficacy of this vaccine (fig 22_A). Fewer dead cells could be detected in the site when animals were vaccinated as compared to not vaccinated or antibiotic treated animals highlighting the power of the vaccine in reducing *S. aureus* mediated cellular toxicity. Moreover, a lower degree in general inflammation could also be detected, since less neutrophils were recruited after infection in vaccinated animals (fig.22_B). This was also evident when proinflammatory cytokines were analyzed in vaccinated and not vaccinated mice (fig.22_C). Most of them resulted indeed slightly reduced in treated animals as compared to controls. Finally, B cell number seemed to be restored in vaccinated animals, but this was also evident for the antibiotic treatment. In this case, probably, a dual role was played. On the one hand systemic protection of immune cells against *S. aureus* toxicity allowed more B cells to survive and to migrate to the tissues and organs where they are requested. On the other hand, local protection against toxicity resulted in a lower killing of B cells. These two aspects could be both present in the vaccinated animals where bacterial reduction *in situ* resulted in a lower local toxicity, while in mice treated with ampicillin only the systemic

component should be responsible for the final outcome. It is in any case difficult to dissect the relative contribution of the two components.

The Novartis vaccine mechanism of protection is nevertheless not completely unraveled. Further analyses are for example necessary for dissecting CD4+ T cells and neutrophils activities. On the basis of the results we have already obtained, we showed that CD4+ T cell recruitment did not significantly changed among vaccinated, not vaccinated and antibiotic treatment, but we did not still analyzed the specific Th pathways of the different groups. Moreover, activation patterns of neutrophils in the different groups could also be of interest in trying to find new possible correlates of protection.

In summary, we described a murine model of *S. aureus* hematogenous arthritis/osteomyelitis that mimics most of the aspects of the human disease including the different clinical phases and the host immune response. Moreover we used this mouse model to test and prove the protection led by Novartis proposed combo vaccine against these diseases and to unravel the induced mechanism of protection. This model provides an important tool for microbiological and other immunological studies on bone and joint infections and for the evaluation of novel approaches for vaccine, diagnostics and therapeutic treatments.

4 Material and Methods

4.1 Bacterial strains

Staphylococcus aureus Xen36 was derived from the parental strain *Staphylococcus aureus* ATCC 49525 (Wright), a clinical isolate from bacteremia patient. *S.aureus* Xen 36 possesses a stable copy of the modified *Photorhabdus luminescens* luxABCDE operon at a single integration site on a native plasmid (87).

Staphylococcus aureus Xen8.1 was derived from the parental strain *S. aureus* 8325-4. *S. aureus* Xen8.1 was engineered through transposition of Tn4001luxABCDE on plasmid pXen-5. Xen8.1 possesses a single stable copy of the modified *P. luminescens* lux operon that was inserted in the δ-toxin coding region in the RNAIII transcript downstream of the agr P3 promoter on chromosome (88).

Staphylococcus aureus Xen29 was derived from the parental strain *S. aureus* 12600, a pleural fluid isolate, which is also designated as NCTC8532. *S. aureus* Xen29 possesses a stable copy of the modified *Photorhabdus luminescens* lux ABCDE operon at a single integration site on the bacterial chromosome (89,90).

S. aureus strain Newman was isolated in 1952 from a human infection (NCTC8178), originally isolated from a case of secondarily infected tubercular osteomyelitis in man and has been used extensively in animal

models of staphylococcal disease due to its robust virulence phenotypes (91).

4.2 Preparation of Bacteria

An aliquot of Bacteria (2ml) frozen in PBS + BSA 10% w/v + glutamate 10% v/v is thawed, inoculated in 48 ml of Triptych Soy Broth (starting from an optical density of 0.05) and incubated at 37°C in agitation (250 RPM). Bacteria were grown until the optical density at 600 nm (OD600), reached OD 2 they were washed twice with sterile PBS and centrifuged at 4000 Xg for 10 minutes. Bacterial pellet was suspended in PBS in order to obtain the desired concentration.

4.3 *In vivo* imaging

For the 2D in vivo imaging acquisitions, IVIS 100® (Perkin Elmer) was used. For 3D in vivo imaging acquisition, The IVIS® SpectrumCT was used. After infection with bioluminescent *S. aureus* Xen 36, Xen 8.1 or Xen 29, mice were anesthetized with isofluorane 2.5% and imaged. Bioluminescent images were displayed using a pseudocolor scale (blue representing the least-intense light and red representing the most-intense light) that was overlaid on a gray-scale image to generate a 2D or 3D picture of the distribution of bioluminescent bacteria in the animal. The acquired image data were saved as two-dimensional arrays containing values corresponding to the number of photons contained within each pixel. The photon emissions from a region of interest (ROI) were quantified

using the Living Image 2.1 software package (Xenogen Corporation), and the data are presented as relative light units contained within each region.

To confirm that the bioluminescence signals corresponded to the bacterial burden *in vivo*, bacteria from knee joint were quantified. The CFU's number of each knee joint was related with its ROI value (photon/second) using the Spearman correlation.

4.4 Histopathology examination

Histologic examination of hind legs at each time point (time 0, 3, 7, 14, 30 90 days post infection) was performed after routine fixation, decalcification, paraffin embedding, and staining with hematoxylin and eosin. Severity and age grade of arthritis/osteomyelitis were assessed by a blinded experienced pathologist analyzing different features of joint and bone diseases (exudate, synovitis, pannus formation, cartilage, bone destruction and deformation, abscesses formation, presence of different characteristic cells) and each slide was graded using a specific scale.

4.5 Immunohistochemistry

Immunohistochemical analysis on 4-µm knee joints sections was performed by using Ventana Benchmark® XT autostainer: primary Anti-*Staphylococcus aureus* antibody conjugated with biotin (ab68954) was diluted 4.5 mg/ml in PBS+BSA 3% and incubated overnight. Negative control slides without primary antibodies were included for each staining. High ionic strength protein blocking solution for reduction of background

was used (Antibody Block Ventana 760-4204). For the antibody detection the DISCOVERY® RedMap Kit (RUO 760-123 250) was used.

4.6 Confocal microscopy

To verify bacterial localization, knee joints of mice infected with 2×10^6 CFU of *S. aureus* and sacrificed one week later, were frozen and then cut using cryostat. Samples were fixed in 2% paraformaldehyde (PFA) for 20 min at room temperature (RT) and then washed three times with a permeabilizing solution containing Bovin Serum Albumin (3%) and Saponin (1%).

The antibody mix solution, composed by anti-osteocalcin (goat) final dilution 1:250, and anti *S. au*reus (rabbit) final dilution 1:200 (both by Abcam) was used to detect the bone and *S. aureus* cells respectively. After 1 h of incubation, the mix with secondary antibodies was added to the knee slide. This mix was composed by chicken anti-goat conjugated with ALEXA FLUOR 647 (far red) final dilution 1:200 to stain osteocalcin, by goat anti-rabbit conjugated with ALEXA FLUOR 488 FITC (green) final dilution 1:200 to stain *S. aureus* cells, and by phalloidin, final dilution 1:300, conjugated with ALEXA FLUOR 568 (red). Secondary antibodies were incubated for 50 min at room temperature (RT).

Samples were washed three times with the permeabilizing solution (BSA 3% and saponin 1%), two times with PBS and two times with water.

Slides were mounted using Mounting medium with DAPI (Life Technologies) and incubated over night at RT.

Images were obtained using a Zeiss LSM 700 confocal microscope (Carl Zeiss).

4.7 Immunization protocol

Five-week-old CD1 mice were immunized intramuscularly with a prime-boost injection (50ul x2) of purified recombinant antigens (10 μg each antigen) adsorbed to aluminum hydroxide adjuvant (alum, 2 mg/mL) in 14 day interval. Control mice received equal amounts of phosphate-buffered saline (PBS) and alum adjuvant. Animals were bled immediately prior to the first immunization, after each immunization and 7 days after the infection, and serum samples and knee joint washes were collected.

4.8 Antibiotic treatment

Pathogen free CD-1, 8 weeks old female mice were infected with Newman strain 1/2 x10^6 via lateral tail vein. 24 and 48 hours after the inoculum mice were treated intraperitoneally with Ampicillin 100 μg/g of body weight, or with PBS (control group).

4.9 Mice and infection model

Pathogen free CD-1, 8 weeks old female mice were purchased from Charles River. Mice were inoculated with *S. aureus* in 100 μL of PBS via lateral tail vein. At each time point blood, kidneys, and hind legs were collected, to perform histological staining, CFU's counting, IgG, IgM, cytokines measurement and multiparameter immune cell flow cytometry.

Mice were monitored on a daily basis and euthanized for humane reasons when they exhibited defined endpoints that had been pre-established for these studies in agreement with the Novartis Animal Welfare Policies. Animal protocols were approved by the Novartis Animal Ethical Committee, Siena, Italy, and the Italian Ministry of Health, Rome, Italy. At each time point 6 mice were sacrificed, 2 of them were dedicated to histology. Kidneys were homogenized using " gentleMACS™ Dissociator " and plated in several dilution on TSB plates.Legs were dissected and muscles excised in order to expose the knee joint. In the joint, between the femur and the tibia, a cut is made with a scalpel. Several washes of this site are performed in 2 ml of RPMI. Suspensions are filtered using a 70 μm nylon mash (Becton Dickinson). An aliquot of these joint washes is used to count CFU, plating it on TSA plates in several dilutions. Blood was collected in presence of heparin (50U/ml). An aliquot is used to count the CFU's number, plating it on TSA plates in several dilutions and 50 μL were lysed (BD Pharm Lyse™), for Flow cytometry staining.

4.10 Antibodies measurements

At each time point of observation serum samples and knee joint washes were examined for IgG and IgM antibodies directed against Hla purified antigen using the Luminex technology. Specifically, 20 μg of recombinant protein was coupled to the carboxyl groups of 2.5 million MicroPlex microspheres (Luminex Corp), according to the manufacturer's instructions. The coupling reaction was confirmed by incubating 5,000

antigen-coupled microspheres with eight serial twofold dilutions of a hyperimmune antiserum used as a reference. To determine serum titers, the beads were incubated with mouse specific sera (dilution 1:10,000 in PBS), washed twice in 200 µl of PBS, and then incubated with phycoerythrin-conjugated secondary antibodies (1:200; Jackson ImmunoResearch) for 15 min in a dark room onto an orbital shaker.

IgG measurements were determined on the Luminex 200 analyzer using Bio-Plex Manager 5.0 software (Bio-Rad, Hercules, CA). Tests were performed in duplicate, and the mean fluorescence intensity (MFI) was determined. The limit of quantification (LOQ) of the assay was determined at an MFI of 100 and was considered the threshold for positive results.

4.11 Cytokine analysis

Joint washes supernatants and serum samples were collected at different time points post infection and cytokine concentrations were measured by multiplex-bead ELISA (Bioplex, BioRad) according to manufacturer's instruction using the mouse 23-plex panel.

The cytokines analyzed were IL-1α, IL-1β, IL-2, IL-3, IL-4, IL-5, IL-6, IL-9, IL-10, IL-12(p40), IL-12(p70), IL-13, IL-17, Eotaxin, G-CSF, GM-CSF, IFN-γ, KC, MCP-1, MIP-α, MIP-1β, RANTES and TNF-α.

4.7 Flow Cytometry staining

Filtered joint washes, and blood were centrifuged (300 Xg, room temperature, 5'). Cell pellets were suspended in 100 µl of PBS and

transferred in 96 wells round bottom plate. Cells were washed twice in PBS (1200 RPM, room temperature, 5') and treated with PBS + CD16/CD32 (FcγIII/II Receptor) to saturate aspecific binding sites and incubated 20', in the dark at room temperature. Cells were stained with combinations of the following antibodies: Ly6g PE, CD11B APC, CD11C APC fluor 780, MHC II Alexa fluor 700, F4/80 V450,LY6C FITC, CD3 PE Cy7, CD19 PECy5, CD4 V500, CD8 PE TEXAS RED, CD335 PERCP Cy 5.5. Antibodies mix solution, prepared in PBS was added at each sample and incubated 20', in the dark at 4°C. 150 μl of PBS is added at each sample and centrifuged (300 XG, 4°C, 5'), two times. 100 μl of CITOFIX is added at each sample and incubated 30', in the dark at 4°C. 150 μl of PBS is added at each sample and centrifuged (350 XG, 4°C, 5'), twice. Cell pellets were suspended in 200 μl PBS/BSA(1%). The stained cells were analyzed using FACS LSR II SOS (special order system, BD) using Flow Jo software 9.3.3 (BD Bioscience).

4.8 Statistical analysis

Statistical analysis were performed using Graph Pad Prism 5 . Wilcoxon-Mann-Whitney test (two tailed) or Spearman, for correlation analysis, were used to calculate statistical significance.

5 Bibliography

1) Classics in infectious diseases. "On abscesses". Alexander Ogston (1844-1929) Rev Infect Dis. 1984 Jan-Feb;6(1):122-8.

2) Ryan KJ, Ray CG. Sherris Medical Microbiology (4th ed.) McGraw Hill (2004)

3) Kluytmans J, van Belkum A, Verbrugh H. "Nasal carriage of Staphylococcus aureus: epidemiology, underlying mechanisms, and associated risks". Clin. Microbiol. Rev. July 1997.10 (3): 505–20.

4) Cimolai N "MRSA and the environment: implications for comprehensive control measures". Eur. J. Clin. Microbiol. Infect. Dis. July 2008. 27 (7): 481–93.

5) Cole, A. M.; Tahk, S.; Oren, A.; Yoshioka, D.; Kim, Y. H.; Park, A.; Ganz, T . "Determinants of Staphylococcus aureus nasal carriage". Clin Diagn Lab Immunol 8.November 2001

6) Yan, Miling; Pamp, Sünje J.; Fukuyama, Julia; Hwang, Peter H.; Cho, Do-Yeon; Holmes, Susan; Relman, David A. "Nasal Microenvironments and Interspecific Interactions Influence Nasal Microbiota Complexity and *S. aureus* Carriage". Cell Host & Microbe December 2013.14 (6): 631–640.

7) Lina, G., Y. Gillet, F. Vandenesch, M. E. Jones, D. Floret, and J. Etienne. Toxin involvement in staphylococcal scalded skin syndrome. Clin. Infect. Dis. 1997. 25:1369–1373.

8) Lina, G., Y. Piemont, F. Godail-Gamot, M. Bes, M. O. Peter, V. Gauduchon, F. Vandenesch, and J. Etienne. Involvement of Panton-

Valentine leukocidin-producing Staphylococcus aureus in primary skin infections and pneumonia. Clin. Infect. Dis. 1999. 29:1128–1132.

9) Jarraud S1, Mougel C, Thioulouse J, Lina G, Meugnier H, Forey F, Nesme X, Etienne J, Vandenesch F. Relationships between Staphylococcus aureus genetic background, virulence factors, agr groups (alleles), and human disease. Infect Immun. 2002 Feb;70(2):631-41.

10) Musser, J. M., P. M. Schlievert, A. W. Chow, P. Ewan, B. N. Kreiswirth, V. T. Rosdahl, A. S. Naidu, W. Witte, and R. K. Selander. A single clone of Staphylococcus aureus causes the majority of cases of toxic shock syndrome. Proc. Natl. Acad. Sci. USA 1990.87:225–229.

11) V. A. Fischetti, R. P. Novick, J. J. Ferretti, D. A. Portnoy, and J. I. Rood.Pathogenicity factors and their regulation in Gram-positive pathogens. American Society for Microbiology, 2000.p.392–407.

12) Broughan J, Anderson R, Anderson AS. Expert Rev Vaccines. Strategies for and advances in the development of Staphylococcus aureus prophylactic vaccines; 2011 May. 10(5):695-708. doi: 10.1586/erv.11.54.

13) Berendt T, Byren I. Bone and joint infection. Clin Med. 2004 Nov-Dec;4(6):510-8.

14) Ciampolini J, Harding KG. Pathophysiology of chronic bacterial osteomyelitis. Why do antibiotics fail so often? Postgrad Med J. 2000 Aug . 76(898):479-83.

15) Goldenberg DL. Septic arthritis. Lancet. 1998 Jan. 17;351(9097):197-202.

16) Lazzarin P, Cesaro G, Puggina S, Perin B, Cremonini L, Padovani G, Sfriso P, Sartori MT Femoral and humeral head osteonecrosis in a patient with hypofibrinolysis and hyperhomocysteinemia. A case report and a review of the literature. Reumatismo. 2004 Jul-Sep; 56(3):202-1017

17) Lew DP, Waldvogel FA Osteomyelitis. Lancet. 2004 Jul 24-30;364(9431):369-79.

18) Klein, R. S. Joint infection, with consideration of underlying disease and sources of bacteremia in hematogenous infection. Clin. Geriatr. Med 1988. 4:375-394.

19) Morgan DS, Fisher D, Merianos A, Currie BJ An 18 year clinical review of septic arthritis from tropical Australia. Epidemiol Infect. 1996 Dec . 117(3):423-8.

20) Nade S. Septic arthritis. Best Pract Res Clin Rheumatol. 2003 Apr. 17(2):183-200.

21) Stott NS. Paediatric bone and joint infection. J Orthop Surg 2001 Jun (Hong Kong).9(1):8390.

22) Levine M, Siegel LB. A swollen joint: why all the fuss? Am J Ther. 2003 May-Jun. 10(3):219.

23) Weichert S, Sharland M, Clarke NM, Faust SN. Acute haematogenous osteomyelitis in children: is there any evidence for how long we should treat? Curr Opin Infect Dis. 2008 Jun. 21(3):258-62. doi: 10.1097/QCO.0b013e3283005441.

24) GALLIE WE. First recurrence of osteomyelitis eighty years after infection. J Bone Joint Surg Br. 1951 Feb. 33-B(1):110-1.

25) Korovessis P, Fortis AP, Spastris P, Droutsas P. Acute osteomyelitis of the patella 50 years after a knee fusion for septic arthritis. A case report. Clin Orthop Relat Res.1991 Nov. 272:205-7.

26) Al Arfaj AS. A prospective study of the incidence and characteristics of septic arthritis in a teaching hospital in Riyadh, Saudi Arabia. Clin Rheumatol. Epub 2008. 27(11):1403-10.

27) Dubost JJ, Soubrier M, De Champs C, Ristori JM, Bussiére JL, Sauvezie B. No changes in the distribution of organisms responsible for septic arthritis over a 20 year period. Ann Rheum Dis. 2002 Mar. 61(3):267-9.

28) Ryan PJ, Fogelman I. Bone scintigraphy in metabolic bone disease. Semin Nucl Med. 1997 Jul. 27(3):291-30.

29) Shirtliff ME, Mader JT. Acute septic arthritis. Clin Microbiol Rev; 2002 Oct. 15(4):527-44.

30) Stott NS. Paediatric bone and joint infection. J Orthop Surg 2001 Jun (Hong Kong). 9(1):83-90.

31) Kwan T.S., Padrines M., Theoleyre S., Heymann D., Fortun Y. IL-6, RANKL, TNF-alpha/IL-1: interrelations in bone resorption pathophysiology. Cytokine Growth Factor Rev. 2004.15:49–60

32) Evans CA1, Jellis J, Hughes SP, Remick DG, Friedland JS. Tumor necrosis factor-alpha, interleukin-6, and interleukin-8 secretion and the acute-phase response in patients with bacterial and tuberculous osteomyelitis. J Infect Dis. 1998 Jun;177(6):1582-7.

33) Klosterhalfen B, Peters KM, Tons C, Hauptmann S, Klein CL, Kirkpatrick CJ.Local and systemic inflammatory mediator release in patients with acute and chronic posttraumatic osteomyelitis. J Trauma. 1996 Mar;40(3):372-8.

34) Osiri M[1], Ruxrungtham K, Nookhai S, Ohmoto Y, Deesomchok U. IL-1beta, IL-6 and TNF-alpha in synovial fluid of patients with non-gonococcal septic arthritis Asian Pac J Allergy Immunol. 1998 Dec;16(4):155-60.

35) Sáez-Llorens X, Mustafa MM, Ramilo O, Fink C, Beutler B, Nelson JD.Tumor necrosis factor alpha and interleukin 1 beta in synovial fluid of infants and children with suppurative arthritis. Am J Dis Child. 1990 Mar;144(3):353-6.

36) Pivirotto LA, Cissel DS, Keeting PE. Sex hormones mediate interleukin-1 beta production by human osteoblastic HOBIT cells. Mol Cell Endocrinol. 1995 Apr 28;111(1):67-74

37) Bost KL, Ramp WK, Nicholson NC, Bento JL, Marriott I, Hudson MC. Staphylococcus aureus infection of mouse or human osteoblasts induces high levels of interleukin-6 and interleukin-12 production. J Infect Dis. 1999 Dec;180(6):1912-20

38) Ishimi Y, Miyaura C, Jin CH, Akatsu T, Abe E, Nakamura Y, Yamaguchi A, Yoshiki S, Matsuda T, Hirano T, et al. IL-6 is produced by osteoblasts and induces bone resorption. J Immunol. 1990 Nov 15;145(10):3297-303.

39) Bacterial infection of osteoblasts induces interleukin-1beta and interleukin-18 transcription but not protein synthesis. Marriott I, Hughes FM Jr, Bost KL. J Interferon Cytokine Res. 2002 Oct;22(10):1049-55

40) Robinson L.J., Borysenko C.W., Blair H.C. Tumor necrosis factor family receptors regulating bone turnover: new observations in osteoblastic and osteoclastic cell lines. Ann. NY Acad. Sci. 2007;1116:432–443.

41) Garzoni C., Kelley W.L. Staphylococcus aureus: new evidence for intracellular persistence. Trends Microbiol. 2009;17:59.

42) Kintarak S, Whawell SA, Speight PM, Packer S, Nair SP. Internalization of Staphylococcus aureus by human keratinocytes. Infect Immun. 2004 Oct;72(10):5668-75.

43) Reilly S.S., Hudson M.C., Kellam J.F., Ramp W.K. In vivo internalization of Staphylococcus aureus by embryonic chick osteoblasts. Bone. 2000;26:63–70.

44) Switalski, L. M., J. M. Patti, W. Butcher, A. G. Gristina, P. Speziale, and M. Hook. A collagen receptor on Staphylococcus aureus strains isolated from patients with septic arthritis mediates adhesion to cartilage. Mol. Microbiol. 1993; 7:99-107

45) Nilsson, I. M., J. M. Patti, T. Bremell, M. Hook, and A. Tarkowski. Vaccination with a recombinant fragment of collagen adhesin provides protection against Staphylococcus aureus-mediated septic death. J. Clin. Investig. 1998;101:2640-2649

46) Thomas, M. G., S. Peacock, S. Daenke, and A. R. Berendt. Adhesion of Staphylococcus aureus to collagen is not a major virulence determinant for septic arthritis, osteomyelitis, or endocarditis. J. Infect. Dis. 1999;179:291-293

47) Peacock, S. J., N. P. Day, M. G. Thomas, A. R. Berendt, and T. J. Foster. Clinical isolates of Staphylococcus aureus exhibit diversity in fnb genes and adhesion to human fibronectin. J. Infect. 2000;41:23-31

48) Hudson, M. C., W. K. Ramp, N. C. Nicholson, A. S. Williams, and M. T. Nousiainen. Internalization of Staphylococcus aureus by cultured osteoblasts. Microb. Pathog. 1995; 19:409-419

49) Lammers, A., P. J. Nuijten, and H. E. Smith. The fibronectin binding proteins of Staphylococcus aureus are required for adhesion to and invasion of bovine mammary gland cells. FEMS Microbiol. Lett. 1999; 180:103-109

50) Ellington, J. K., S. S. Reilly, W. K. Ramp, M. S. Smeltzer, J. F. Kellam, and M. C. Hudson. Mechanisms of Staphylococcus aureus invasion of cultured osteoblasts. Microb. Pathog. 1999;26:317-323

51) Bayles, K. W., C. A. Wesson, L. E. Liou, L. K. Fox, G. A. Bohach, and W. R. Trumble. Intracellular Staphylococcus aureus escapes the endosome and induces apoptosis in epithelial cells. Infect. Immun. 1998; 66:336-342

52) Menzies, B. E., and I. Kourteva. Internalization of Staphylococcus aureus by endothelial cells induces apoptosis. Infect. Immun 1998; 66:5994-5998

53) Wesson, C. A., J. Deringer, L. E. Liou, K. W. Bayles, G. A. Bohach, and W. R. Trumble. Apoptosis induced by Staphylococcus aureus in epithelial cells utilizes a mechanism involving caspases 8 and 3. Infect. Immun. 2000; 68:2998-3001-).

54) Gresham, H. D., J. H. Lowrance, T. E. Caver, B. S. Wilson, A. L. Cheung, and F. P. Lindberg. Survival of Staphylococcus aureus inside neutrophils contributes to infection. J. Immunol. 2000;164:3713-3722

55) Mark E. Shirtliff1 and Jon T. Mader. Acute Septic Arthritis Clin Microbiol Rev. Oct 2002; 15(4): 527–544.

56) Henderson B., Nair S.P. Hard labour: bacterial infection of the skeleton. Trends Microbiol. 2003;11:570

57) Von Eiff C, Bettin D, Proctor RA, Rolauffs B, Lindner N, Winkelmann W, Peters G. Recovery of small colony variants of Staphylococcus aureus following gentamicin bead placement for osteomyelitis. Clin Infect Dis. 1997 Nov;25(5):1250-1

58) Mishra RP, Mariotti P, Fiaschi L, Nosari S, Maccari S, Liberatori S, Fontana MR, Pezzicoli A, De Falco MG, Falugi F, Altindis E, Serruto D, Grandi G, Bagnoli F. Staphylococcus aureus FhuD2 is involved in the early phase of staphylococcal dissemination and generates protective immunity in mice. J Infect Dis. 2012 Oct 1;206(7):1041-9.

59) Frank KM1, Zhou T, Moreno-Vinasco L, Hollett B, Garcia JG, Bubeck Wardenburg J. Host response signature to Staphylococcus aureus alpha-hemolysin implicates pulmonary Th17 response. Infect Immun. 2012 Sep;80(9):3161-9.

60) Menzies BE1, Kernodle DS. Site-directed mutagenesis of the alpha-toxin gene of Staphylococcus aureus: role of histidines in toxin activity in vitro and in a murine model. Infect Immun. 1994 May. 62(5):1843-7.

61) Burts ML, Williams WA, DeBord K, Missiakas DM. EsxA and EsxB are secreted by an ESAT-6-like system that is required for the pathogenesis of Staphylococcus aureus infections. Proc Natl Acad Sci USA. 2005;102:1169–1174

62) Francis KP, Joh D, Bellinger-Kawahara C, Hawkinson MJ, Purchio TF, Contag PR. Monitoring bioluminescent Staphylococcus aureus infections in living mice using a novel luxABCDE construct. Infect Immun; 2000 Jun. 68(6):3594-600.

63) Meighen EA. Molecular biology of bacterial bioluminescence. Microbiol Rev; 1991 Mar. 55(1):123-42.

64) Cheng AG, Kim HK, Burts ML, Krausz T, Schneewind O, Missiakas DM Genetic requirements for Staphylococcus aureus abscess formation and persistence in host tissues. FASEB J. 2009 Oct;23(10):3393-404.

65) Darley ES1, MacGowan AP. Antibiotic treatment of gram-positive bone and joint infections. J Antimicrob Chemother. 2004 Jun. 53(6):928-35.

66) Mal P1, Ghosh D, Bandyopadhyay D, Dutta K, Bishayi B. Ampicillin alone and in combination with riboflavin modulates Staphylococcus aureus infection induced septic arthritis in mice. Indian J Exp Biol; 2012 Oct. 50(10):677-89.

67) Bhakdi S, Tranum-Jensen J (December 1991). α-toxin of Staphylococcus aureus". Microbiol. Rev. 55 (4): 733–51.

68) Tarkowski A1, Collins LV, Gjertsson I, Hultgren OH, Jonsson IM, Sakiniene E, Verdrengh M.18   Morgan, D.S. et al. Model systems: modeling human staphylococcal arthritis and sepsis in the mouse. Trends Microbiol. 2001 Jul;9(7):321-6.

69) Patel M , Rojavin Y , Jamali AA , Wasielewski SJ , Salgado CJ . Animal models for the study of osteomyelitis. SeminPlastSurg. 2009;23:148–154

70) Funao H, Ishii K, Nagai S, Sasaki A, Hoshikawa T, Aizawa M, et al. Establishment of a real-time, quantitative, and reproducible mouse model of Staphylococcus osteomyelitis using bioluminescence imaging. Infect Immun . 2012;80:733–741

71) Li D, Gromov K, Søballe K, Puzas JE, O'Keefe RJ, Awad H, et al. Quantitative mouse model of implant-associated osteomyelitis and the kinetics of microbial growth, osteolysis, and humoral immunity. J Orthop Res . 2008;26:96–105

72) Horst SA, Hoerr V, Beineke A, et al. A novel mouse model of Staphylococcus aureus chronic osteomyelitis that closely mimics the human infection: an integrated view of disease pathogenesis. Am J Pathol. 2012;181(4):1206–1214.

73) T. Bremell, S. Lange, A. Yacoub, C. Rydén, and A. Tarkowski Experimental Staphylococcus aureus arthritis in mice. Infect Immun. Aug 1991; 59(8): 2615–2623.

74) Belthur MV, Birchansky SB, Verdugo AA, Mason EO, Hulten KG, Kaplan SL, et al. Pathologic fractures in children with acute Staphylococcus aureus osteomyelitis . J bone Joint Surg Am . 2012;94:34–42

75)Jones HW , Beckles VL , Akinola B , Stevenson AJ , Harrison WJ . Chronic haematogenous osteomyelitis in children: an unsolved problem . J bone Joint Surg Br . 2011;93:1005–1010

76) Herrmann, M., P. E. Vaudaux, D. Pittet, R. Auckenthaler, P. D. Lew, F.Schumacher-Perdreau, G. Peters, and F. A. Waldvogel. Fibronectin, fibrinogen, and laminin act as mediators of adherence of clinical staphylo-coccal isolates to foreign material. J. Infect. Dis. 1988. 158:693–701

77) Patti JM1, Jonsson H, Guss B, Switalski LM, Wiberg K, Lindberg M, Höök M.70) Ryden, C., I. Maxe, A. Franzen, A. Ljungh, D. Heinegard, and K. Rubin. Molecular characterization and expression of a gene encoding a Staphylococcus aureus collagen adhesin. J Biol Chem. 1992 Mar 5;267(7):4766-72.

78) Rydén C, Maxe I, Franzén A, Ljungh A, Heinegård D, Rubin K.Lancet. Selective binding of bone matrix sialoprotein to Staphylococcus aureus in osteomyelitis. 1987 Aug 29;2(8557):515.

79) Verdrengh M1, Tarkowski A. Role of macrophages in Staphylococcus aureus-induced arthritis and sepsis. Arthritis Rheum. 2000 Oct;43(10):2276-82.

80) Verdrengh M1, Tarkowski A. Role of neutrophils in experimental septicemia and septic arthritis induced by Staphylococcus aureus. Infect Immun. 1997 Jul;65(7):2517-21.

81) Arend WP, Dayer JM. Cytokines and cytokine inhibitors or antagonists in rheumatoid arthritis. Arthritis Rheum. 1990 Mar;33(3):305-15.

82) Abdelnour A, Bremell T, Holmdahl R, Tarkowski A. Clonal expansion of T lymphocytes causes arthritis and mortality in mice infected with toxic shock syndrome toxin-1-producing staphylococci. Eur J Immunol. 1994 May;24(5):1161-6.

83) Silverman, G.J., and C.S. Goodyear. 2002. A model B-cell superantigen and the immunobiology of B lymphocytes. Clin. Immunol.102:117–134.

84) Graille, M., E.A. Stura, A.L. Corper, B.J. Sutton, M.J. Taussig, J.B. Charbonnier, and G.J. Silverman. 2000. Crystal structure of a Staphylococcus aureus protein A domain complexed with the Fab fragment of a human IgM antibody: structural basis for recognition of B-cell receptors and superantigen activity. Proc. Natl. Acad. Sci. USA.97:5399–5404

85) Cary, S.P., J. Lee, R. Wagenknecht, and G.J. Silverman. 2000. Characterization of superantigen-induced clonal deletion with a novel clan III-restricted avian monoclonal antibody: exploiting evolutionary distance to create antibodies specific for a conserved VH region surface. J. Immunol.164:4730–4741.

86) Death by a B Cell Superantigen: In Vivo VH-targeted Apoptotic Supraclonal B Cell Deletion by a Staphylococcal Toxin Carl S. Goodyear and Gregg J. Silverman

87) Kelli L. Palmer, Lindsay M. Aye, and Marvin Whiteley Nutritional Cues Control Pseudomonas aeruginosa Multicellular Behavior in Cystic Fibrosis Sputum. Journal of Bacteriology,2007,8079-8087,Vol.189,No.22

88) Kuklin NA1, Pancari GD, Tobery TW, Cope L, Jackson J, Gill C, Overbye K, Francis KP, Yu J, Montgomery D, Anderson AS, McClements W, Jansen KU. Real-time monitoring of bacterial infection in vivo: development of bioluminescent staphylococcal foreign-body and deep-thigh-wound mouse infection models. Antimicrobial Agents and Chemotherapy, Sept. 2003, Vol. 47 No. 9, p. 2740–2748

89) Kadurugamuwa JL1, Sin L, Albert E, Yu J, Francis K, DeBoer M, Rubin M, Bellinger-Kawahara C, Parr Jr TR Jr, Contag PR.Direct continuous method for monitoring biofilm infection in a mouse model. Infection & Immunity, Feb. 2003, Vol. 71, No. 2, pp. 882–890

90) Kadurugamuwa JL, Sin LV, Yu J, Francis KP, Kimura R, Purchio T, Contag PR. Rapid direct method for monitoring antibiotics in a mouse model of bacterial biofilm infection Antimicrobial Agents and Chemotherapy, Oct. 2003, Vol. 47, No. 10, p. 3130–3137

91) DTJTHIE, E. S. & LORENZ, L. L. (1952). Staphylococcal Coagulase: Mode of Action and Antigenicity J. gen. Microbial. 6, 95-107